



NOAA Technical Memorandum NMFS-AFSC-388

# Freshwater Input to the Bering Sea, 1950–2017

K. A. Kearney

**U.S. DEPARTMENT OF COMMERCE**  
National Oceanic and Atmospheric Administration  
National Marine Fisheries Service  
Alaska Fisheries Science Center

February 2019

## NOAA Technical Memorandum NMFS

The National Marine Fisheries Service's Alaska Fisheries Science Center uses the NOAA Technical Memorandum series to issue informal scientific and technical publications when complete formal review and editorial processing are not appropriate or feasible. Documents within this series reflect sound professional work and may be referenced in the formal scientific and technical literature.

The NMFS-AFSC Technical Memorandum series of the Alaska Fisheries Science Center continues the NMFS-F/NWC series established in 1970 by the Northwest Fisheries Center. The NMFS-NWFSC series is currently used by the Northwest Fisheries Science Center.

This document should be cited as follows:

Kearney, K. A. 2019. Freshwater input to the Bering Sea, 1950–2017. U.S. Dep. Commer., NOAA Tech. Memo. NMFS-AFSC-388, 46 p.

Document available: <https://www.afsc.noaa.gov/Publications/AFSC-TM/NOAA-TM-AFSC-388.pdf>

Reference in this document to trade names does not imply endorsement by the National Marine Fisheries Service, NOAA.



NOAA Technical Memorandum NMFS-AFSC-388

# Freshwater Input to the Bering Sea, 1950–2017

K. A. Kearney

Alaska Fisheries Science Center  
Resource Ecology and Fisheries Management Division  
7600 Sand Point Way N.E.  
Seattle, WA 98115

Current affiliation: University of Washington  
College of the Environment  
Joint Institute for the Study of the Atmosphere and Ocean  
3737 Brooklyn Ave NE  
Seattle, WA 98195-5672

*[www.afsc.noaa.gov](http://www.afsc.noaa.gov)*

## **U.S. DEPARTMENT OF COMMERCE**

Wilbur L. Ross Jr., Secretary

### **National Oceanic and Atmospheric Administration**

RDML Timothy Gallaudet (ret.), Acting Under Secretary and Administrator

### **National Marine Fisheries Service**

Chris Oliver, Assistant Administrator for Fisheries

February 2019

**This document is available to the public through:**

National Technical Information Service  
U.S. Department of Commerce  
5285 Port Royal Road  
Springfield, VA 22161

*[www.ntis.gov](http://www.ntis.gov)*

## **ABSTRACT**

We present a new dataset of freshwater river input to the Bering Sea, spanning the years of 1950 to the present (2017). The dataset uses river discharge values measured at stream gauges throughout Alaska and Russia to reconstruct freshwater input to the Bering Sea. This dataset strives to capture the full seasonal variation in streamflow that is seen in this region, where the majority of a river's streamflow occurs in the summer; this seasonal range in values is missing from many common river datasets used in global climate modeling.



# CONTENTS

<b>Introduction</b>	<b>1</b>
<b>Methods</b>	<b>2</b>
Seasonal and Interannual Variability in a Previously-existing River Runoff Dataset	2
Reconstruction of Interannual Streamflow . . . . .	5
Alaska . . . . .	6
Russia . . . . .	8
Future Updates to the Dataset . . . . .	8
Integration Into Bering 10K ROMS Model . . . . .	9
<b>Results and Discussion</b>	<b>10</b>
<b>Appendix: Details of Individual River Reconstructions</b>	<b>17</b>
Hook Point-Frontal Gulf of Alaska . . . . .	19
Resurrection Bay-Frontal Gulf of Alaska . . . . .	20
Nuka Bay-Frontal Gulf of Alaska . . . . .	21
Prince William Sound . . . . .	22
Cape Uganik-Shelikof Strait . . . . .	23
Sevenmile Beach-Frontal Shelikof Strait . . . . .	24
Alitak Bay-Frontal Pacific Ocean . . . . .	25
Tonki Cape Peninsula-Frontal Marmot Bay . . . . .	26
Chiniak Bay . . . . .	27
Sacramento River-Frontal Pacific Ocean . . . . .	28
Sutwik Island-Pacific Ocean . . . . .	29
Cook Inlet . . . . .	30
Unga Island-Frontal Pacific Ocean . . . . .	31

Deer Island . . . . .	32
190301030000 . . . . .	33
Kvichack Bay-Frontal Bristol Bay . . . . .	34
190303060902-Frontal Nushagak Bay . . . . .	35
Ugchirnak Mountain-Frontal Hazen Bay . . . . .	36
Warehouse Bluff-Frontal Kuskokwim Bay . . . . .	37
Taket Creek-Frontal Norton Sound . . . . .	38
Quartz Creek-Frontal Norton Sound . . . . .	39
Crete Creek-Frontal Bering Sea . . . . .	40
King River-Frontal Bering Sea . . . . .	41
Kotzebue Sound . . . . .	42
Outlet Yukon River-Frontal Bering Sea . . . . .	43
Kamchatka River . . . . .	44
Avacha River . . . . .	45
Anadyr River . . . . .	46

## INTRODUCTION

The Bering Sea is a highly productive ecosystem that is home to diverse populations of plankton, fish, birds, and marine mammals, and supports several major commercial fisheries. The region is characterized by a broad southeastern shelf that includes three distinct biophysical domains. While wind and tidal mixing are the predominant forces determining the physical structure of the water in this region, coastal freshwater input can also play a key role. Along the southeastern shelf, plumes of relatively warm fresh water can inhibit mixing along the front separating the inner (0 m to 50 m, shallow, and well-mixed throughout the year) and middle (50 m to 100 m, seasonally stratified) domains (Kachel et al. 2002). Farther north, the Yukon River discharges relatively warm, turbid, nutrient-poor water that pushes coastal waters offshore, maintaining low production regions within the Norton Sound region relative to the colder, more nutrient-rich waters of the offshore Anadyr water mass (Dean et al. 1989).

The annual freshwater discharges associated with the major tributaries of the Bering Sea are high; at least five rivers (the Yukon, Kuskokwim, Susitna, Anadyr, and Copper rivers) average a discharge over  $5 \times 10^4 \text{ ft}^3/\text{s}$ . However, these flow rates have a high seasonal variability, with flow concentrated during the summer months due to snowmelt, glacier melting, and rainfall, and relatively low discharge during the winter months. For example, the Yukon discharges only approximately  $1.05 \times 10^4 \text{ ft}^3/\text{s}$  during the winter, but can exceed  $1 \times 10^6 \text{ ft}^3/\text{s}$  during peak flow.

Under the Bering Sea Integrated Ecosystem Research Project (BSIERP), an implementation of the Regional Ocean Modeling System (ROMS) was built for this region. The model, referred to herein as the Bering 10K model, is able to simulate the primary features of the biophysical domains described above, and has been successfully used to investigate both the physical and biological dynamics of this region (Hermann et al. 2013). These studies focused primarily on the southeast Bering Sea shelf, where freshwater in-

put is a minor driver, and therefore were able to rely on a monthly climatological river runoff dataset designed for the larger northeast Pacific NEP5 ROMS domain (Danielson et al. 2011). However, the Bering 10K model is now being further developed for use in the northern Bering Sea region. In this region, it is much more important that the river forcing dataset used captures both the seasonal and interannual variations in the discharge of warm, fresh water into the model domain.

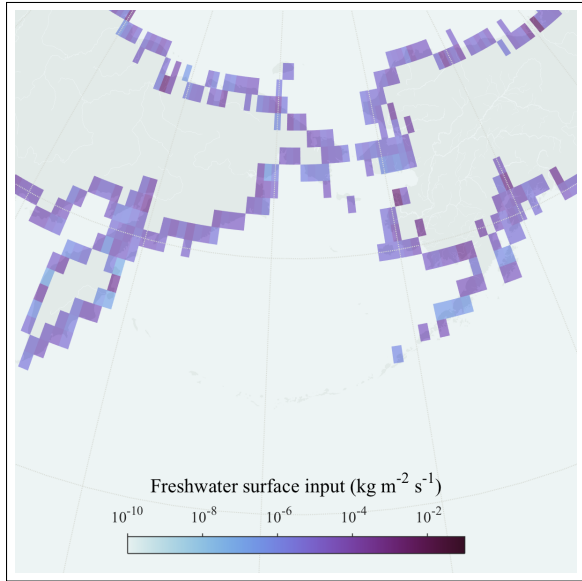
This report details the construction of the new river runoff dataset for the Bering Sea and western Gulf of Alaska watersheds. The final runoff dataset is tailored for use as an input forcing file for the Bering 10K domain ROMS model; however, the intermediate watershed streamflow data, discussed in *Reconstruction of Interannual Streamflow*, may also be informative outside this narrow context.

## METHODS

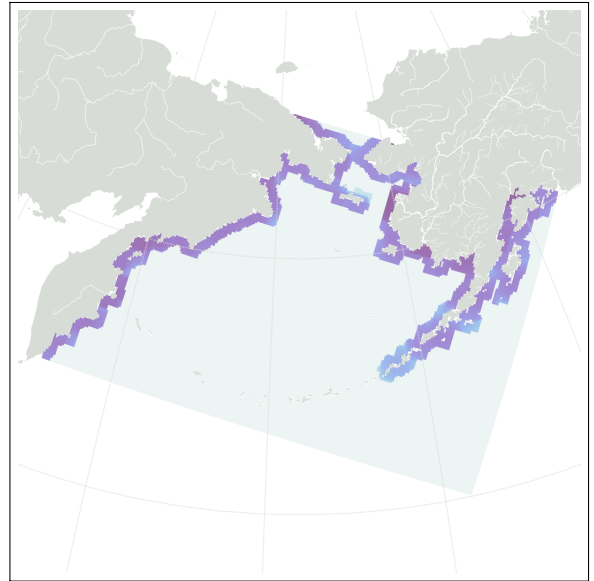
### Seasonal and Interannual Variability in a Previously-existing River Runoff Dataset

Previous versions of the Bering 10K model relied on a downscaled version of the Dai and Trenberth (2002) dataset for its freshwater input values. This dataset provides global monthly mean freshwater discharge values at a 1-degree resolution, based on data from 921 of the world’s largest rivers. It was designed to provide estimates of continental discharge for global climate models. However, there are a few shortcomings associated with this dataset that make it less than ideal for use in the high-resolution Bering Sea model.

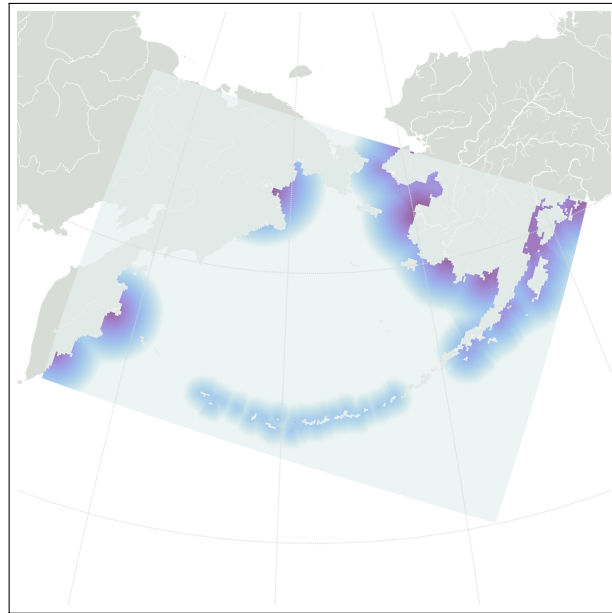
First, the 1-degree resolution of the Dai and Trenberth (2002) dataset is an order of magnitude coarser than that of our 10-km ROMS domain resolution. Features that may play a key role in the physical dynamics of our ocean model, including the plumes of the Yukon and Kuskokwim Rivers, are poorly captured at this resolution (Fig. 1a), even if up-sampled to the model’s resolution (Fig. 1b).



(a) Dai and Trenberth dataset



(b) NEP model



(c) This study

Figure 1. — Surface freshwater flux due to river runoff, based on a) the original Dai and Trenberth (2002) dataset, b) the NEP model version used in previous Bering 10K simulations (the Dai and Trenberth (2002) dataset rescaled to our model grid), and c) this study. Each subpanel shows values averaged over the time period available for each dataset. Note that the rectangular region covered by the latter two indicates the location of the Bering 10K model domain.

Secondly, the Dai and Trenberth (2002) dataset only runs through 2007, while many of the Bering 10K simulations focus on more recent years. To compensate for the missing data, a climatological average across all years was calculated and used in place of the interannual time series for early runs of the Bering 10K model. However, we would prefer to maintain the interannual variability that may play a key role in determining spatial variability in both physical and biological processes in our simulations.

In addition to these issues of spatial and temporal resolution, the Dai and Trenberth (2002) data include some periods of time where the observed seasonal variability between low-discharge winter months and high-discharge summer months is absent. Dai and Trenberth (2002) incorporates composite runoff fields from the world's largest rivers (Fekete et al. 2002); the composites combine data from river gauging stations with simulated estimates of runoff from ungauged regions. We assume that the lack of seasonal variability we see is an artifact of the ungauged runoff reconstruction process used, which may not be appropriate for regions like this one where seasonal variability is high. Figure 2 highlights the time series from one grid cell of the Dai and Trenberth (2002) dataset, alongside the river discharge data from USGS monitoring stations located upstream of this grid cell. It is clear from this comparison that the dataset reflects the true seasonal variability of the Nushagak River over the period of time when a river gauge was active on that river, but switches to a pattern with much lower variability and higher winter streamflow during years when observations are absent at that particular gauge. Note that the Nuyakuk River is a major tributary of the Nushagak, and its longer record does not suggest any major shifts in winter streamflow over time.

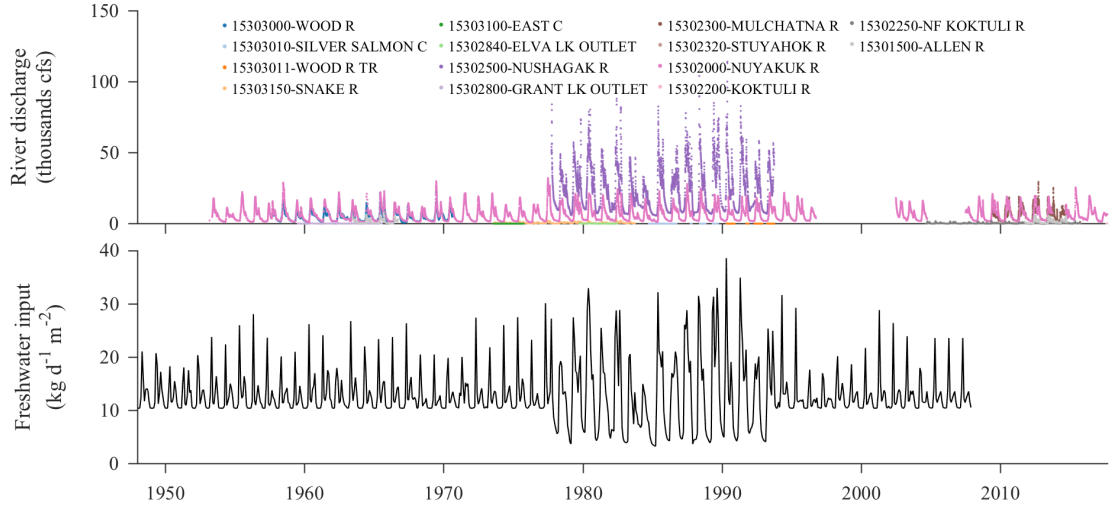


Figure 2. -- The seasonal variability artifact in the Dai and Trenberth (2002) dataset can be seen by examining the time series of fresh water input flux from that dataset within a single grid cell (bottom panel), located near the mouth of the Nushagak River. The top panel shows the raw discharge values measured at all stream gauges located within the Nushagak Bay watershed.

## Reconstruction of Interannual Streamflow

The goal of this river discharge reconstruction is to build a time series of river-derived freshwater input to the Bering Sea and western Gulf of Alaska (i.e. the region covered by the Bering 10K model domain), covering the time period from 1950 to the present, and at a spatial resolution appropriate to the 10-km resolution of the model. *Alaska* and *Russia* present an overview of the river discharge timeseries reconstruction for rivers in both the United States and Russia, respectively. *Integration Into Bering 10K ROMS Model* then describes how these time series were converted to a spatially-varying freshwater input flux, appropriate for use as part of the surface boundary conditions for a ROMS model.

## Alaska

For the eastern side of our model domain, we collected data from the U.S. Geological Survey’s (USGS) National Water Information System (NWIS) surface water database (United States Geological Survey 2016), which archives measurements from stream gauges throughout the United States.

To determine which river gauges to include in this analysis, we began by examining hydrologic units from the Watershed Boundary Dataset (Watershed Boundary Dataset 2017). We based our analysis on the level 12 (subwatershed) hydrologic units from region 19 (Alaska). We began by isolating all hydrologic units that fell within our model domain and drained directly into the ocean rather than to another unit, as indicated by the ToHUC code attached to each hydrologic unit. In this document, we will refer to these ocean-emptying hydrologic units as river mouth units. Each hydrologic unit polygon includes information regarding which other polygon it empties into, and we used this data to trace the network of upstream units whose runoff eventually led to each of the river mouth units; the collection of units associated with each river mouth unit is considered its watershed for the purposes of this study (Fig. 3).

The metadata for each USGS gauging station includes the 8-digit hydrologic unit in which it is located, so we were able to narrow our query of the USGS gauging stations to only those that fell within our watershed boundaries and that included discharge data at some point between 1 January, 1950 and the present. We then further calculated the 12-digit hydrologic unit into which each remaining station fell, using its site location coordinates and the boundary coordinates for each WBD polygon.

Once we had defined our watersheds and the river gauge stations located in each, we began the process of reconstructing streamflow that emptied into each river mouth unit. Ideally, we wanted to collect data from every river that emptied directly into the river mouth unit (or into the frontal units that often form a boundary between the river mouth

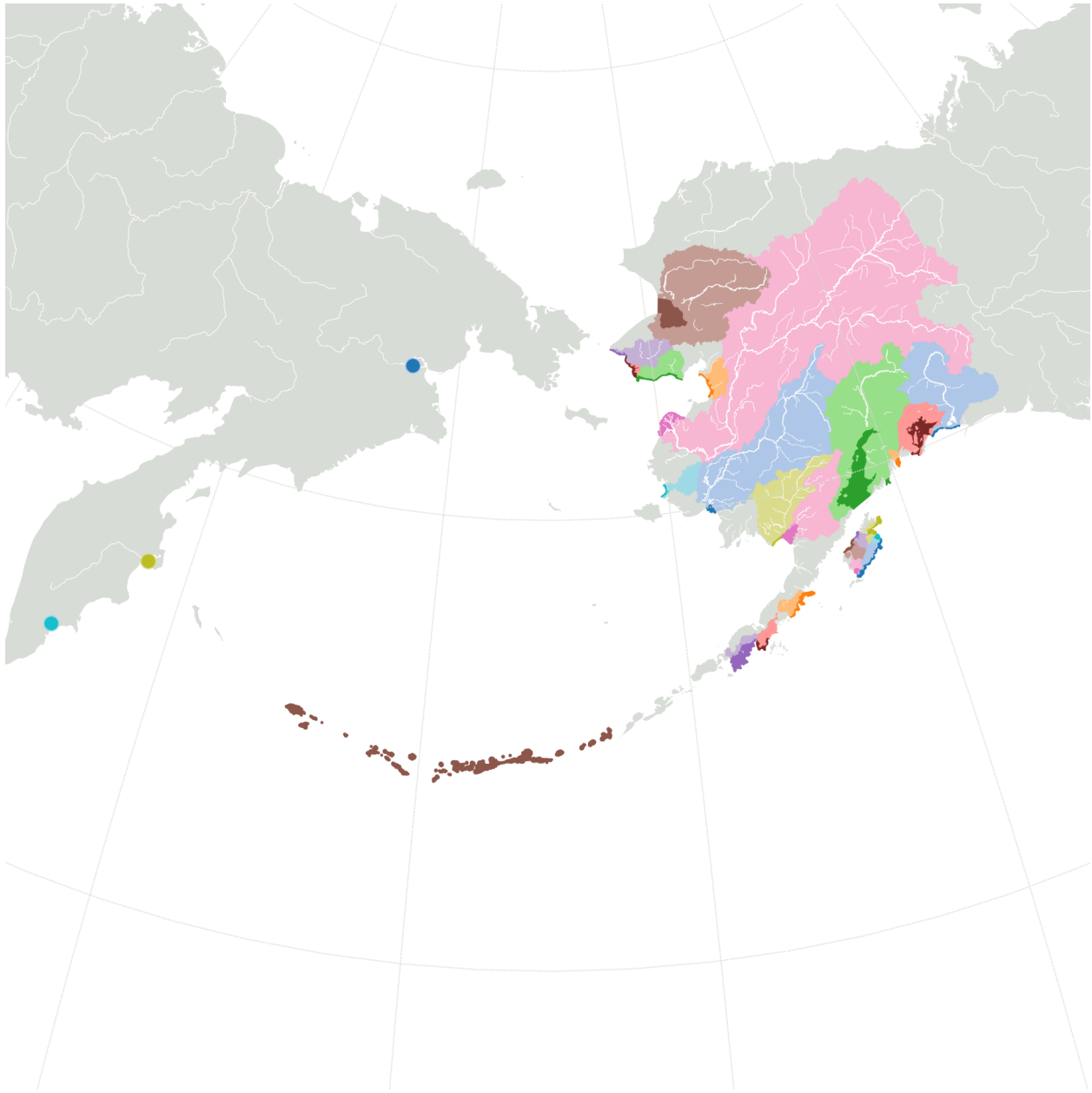


Figure 3. -- This map indicates the watersheds that included at least one USGS streamflow gauge. The darker-colored polygons located along the coasts indicate the river mouth hydrologic units, with the lighter color shaded regions corresponding to the watershed drainage basins associated with each. Russian rivers are indicated by a single point at the mouth of each river. Colors are for contrast only and do not indicate any particular property of each watershed.

unit and more inland units in the same bay or estuary), using a river gauge station that was located downstream of all major tributaries of each river. This ideal situation is com-

plicated by the fact that many rivers are ungauged, some gauges have been discontinued over time and replaced by ones further up- or downstream, and many gauges only include data for a handful of years, with the most continuous records usually located in easy-to-maintain areas that may be upstream of major tributaries. While the process of associating river gauges with each watershed was automated, choosing which river gauges best represented the discharge emptying into each runoff unit involved a manual examination. See the appendix for a full description of the river-choosing decision process behind each watershed in our domain, and the steps taken to extend each river's time series to the full period of interest (1950 - present) if measured data were not available throughout the entire period. Once a full 1950-present time series had been reconstructed for each gauged river emptying into the domain, these values were added together to create a single time series per watershed. Finally, the time series were averaged across monthly bins to match our desired temporal resolution for the ROMS model.

## **Russia**

The western side of the Bering Sea is bordered by Russia. Data sources for river input from this side of the domain are much more limited than on the eastern side of the domain. We retrieved a compilation of monthly streamflow data from stream gauges throughout the former Soviet Union (Bodo 2000), which included time series from the three largest Russian tributaries to the Bering Sea: the Anadyr, Kamchatka, and Avacha rivers. Missing data were filled in using a climatological cycle based on the available data for each of the three rivers.

## **Future Updates to the Dataset**

While the construction of this dataset did require some manual perusing of the available data (see the appendix), the majority of the calculations are automated. Code that can be used to reproduce the calculations and extend them further into the future as new

data becomes available can be found on GitHub: <https://github.com/kakearney/beringriver-pkg>. This includes code to download data remotely from the USGS NWIS database and load data from a local copy of the Bodo (2000) dataset, combine data from the chosen stations into individual river and watershed time series, and horizontally distribute the streamflow across a specified ROMS grid domain. It also includes functions to query the data available from all USGS stations within the Bering Sea watershed to determine if stations used in our analysis have been discontinued or if new stations have been added; this analysis should probably be repeated regularly when extending the dataset to ensure that the choice of data sources remains optimal.

## Integration Into Bering 10K ROMS Model

The Bering 10K ROMS model adds river runoff as a spatially-dependent surface flux of freshwater, similar to precipitation. We distributed each watershed time series across the model grid by weighting each non-land-masked grid cell in the model domain by its distance from either the river mouth hydrologic unit polygon (for the eastern side of the domain) or the point coordinate of the river mouth (for the western side of the domain), assuming exponential decay of river influence and an e-folding scale of 20 km. Weights were normalized to sum to 1 across the entire domain for each river. Streamflow values from each river were then allocated across each grid cell based on these weights, and divided by the spatial area of each grid cell. The result is a gridded time series of freshwater input, in units of  $\text{kg m}^{-2} \text{s}^{-1}$  (Fig. 1c).

To analyze the effects of the new runoff dataset on Bering Sea circulation, we ran a pair of five-year Bering 10K simulations, spanning 1970 - 1975, a time period that represents the beginning of our hindcast forcing dataset. The Bering 10K domain is horizontally resolved at approximately 10 km, with 10 vertical sigma-coordinate depth levels. Bathymetry is derived from ETOPO5 as adjusted for the NEP-5 model domain (Danielson et al. 2011), with smoothing for numerical stability. Winds, air temperature, relative

humidity, and downward shortwave and longwave radiation from the common ocean reference experiment reanalysis (CORE) were used as bulk forcings to constrain surface stress and heat exchanges at the surface boundary (Large and Yeager 2009). The first simulation included runoff-as-precipitation forcing identical to those used in the Hermann et al. (2013) simulations (i.e. a downscaled version of the Dai and Trenberth (2002) dataset). The second simulation used the dataset described in this report.

## RESULTS AND DISCUSSION

Along the U.S. coast on the eastern side of the Bering Sea, we were able to reconstruct time series of freshwater flux that covers the majority of the coastline. The unmonitored stretches of coastline accounted for only a very small percentage of the land in the Bering Sea watershed.

Our reconstruction of the western side of the domain was not as thorough as on the eastern side. We were unable to obtain detailed hydrographic data mapping the watersheds and drainage patterns on this coast, and instead relied only on streamflow from the largest rivers. In particular, the stretch of land between the Anadyr and Kamchatka rivers does not receive any freshwater flux in our dataset, despite the topography of the land suggesting that several small rivers lead to the Bering Sea in this location. The Dai and Trenberth (2002) dataset includes relatively high runoff values here. However, the narrow shelf and deep mixing along this side of the domain relative to the east side means that this lack of data has only a small influence on the overall physical properties in our model simulations. Because the majority of the model simulations are focused on the eastern side of the domain, we have decided that this dataset is sufficient. However, we hope to add a more rigorous river analysis to the western coast, similar to that detailed in the appendix for the eastern coast, should any data become available from this region.

When forced with the new rivers dataset as compared to the older rivers dataset, the most noticeable changes in the physical properties of the Bering 10K model can be seen

in the Norton Sound area. The influence of the Yukon River is much stronger in this shallow region in the new-river simulation compared to the old-river simulation, resulting in less saline conditions, particularly in the summer months (Figs. 4 and 5). This leads to a correspondingly shallower mixed layer depth during the summer months (Fig. 6). The influence of the rivers on salinity is similar but less pronounced along the southeast shelf near Bristol Bay; this is also consistent with observations.

Along the narrow western Bering Sea shelf, we see the opposite pattern, with higher salinity and deeper mixed layer depths in the new-river simulation along the shelf between the Anadyr and Kamchatka river mouths, particularly in the winter and early spring. This may simply be an artifact of the lack of river data we have in this region; however, we currently lack observational data from this side of the domain to validate whether the higher freshwater flux seen in the Dai and Trenberth (2002) dataset in this region reflects the true conditions.

Overall, this new dataset successfully accomplishes our goal to better capture the observed seasonal and interannual variability in Bering Sea salinity due to freshwater discharge from rivers. We note that our current method incorporating runoff as precipitation lacks the ability to add a temperature signal to the freshwater flux. The relatively warmer temperature associated with river runoff is an observed characteristic of the Yukon River plume in particular. Future improvements to this river dataset will develop methods of adding this potentially important property to the freshwater input.

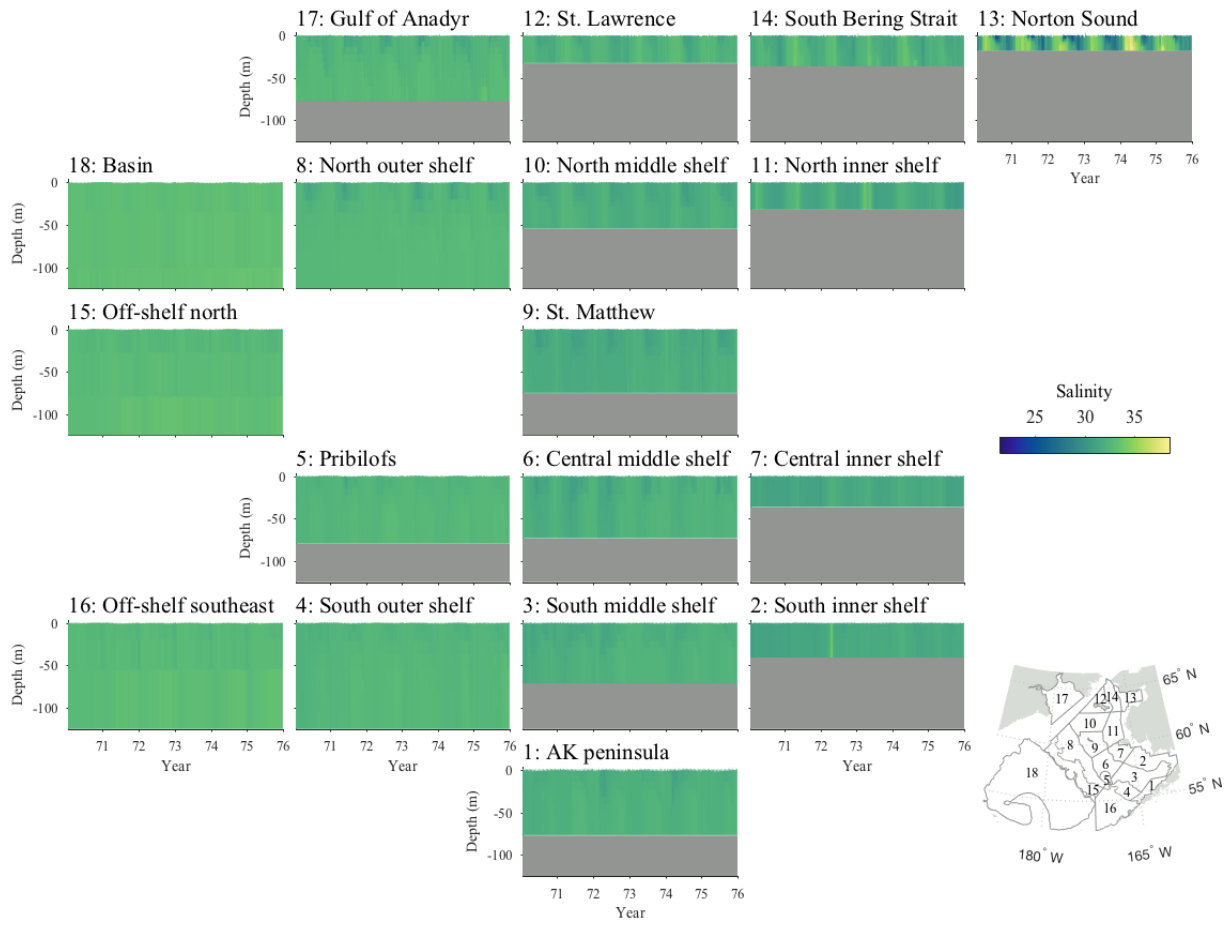


Figure 4. — Salinity over time in the new-rivers simulation. Data were extracted from the model at locations representative of the main biophysical domains along the Bering Sea shelf; the grey shaded portion indicates the water depth at each location.

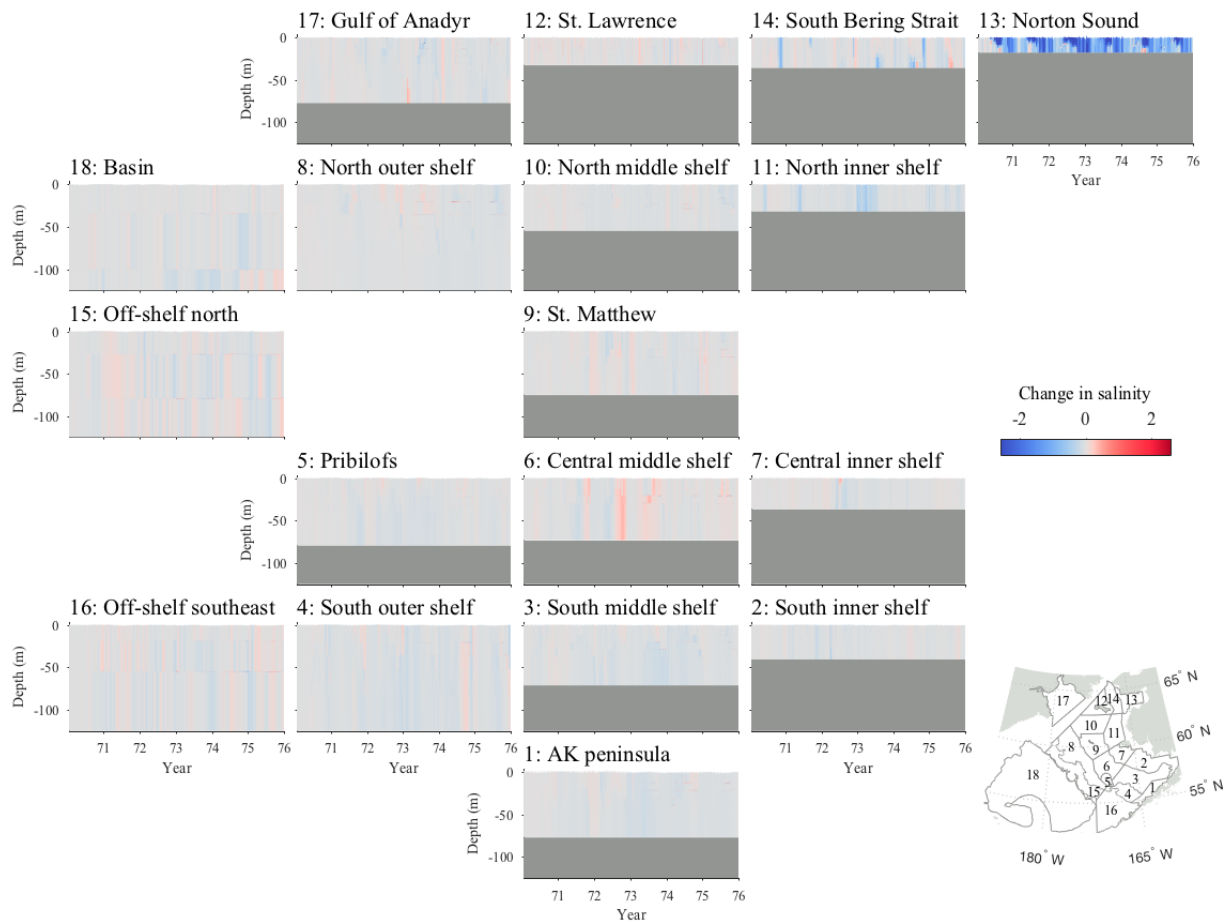


Figure 5. — Change in salinity in the new-rivers simulation relative to the old-rivers simulation. Data was extracted from the model at locations representative of the main biophysical domains along the Bering Sea shelf; the grey shaded portion indicates the water depth at each location.

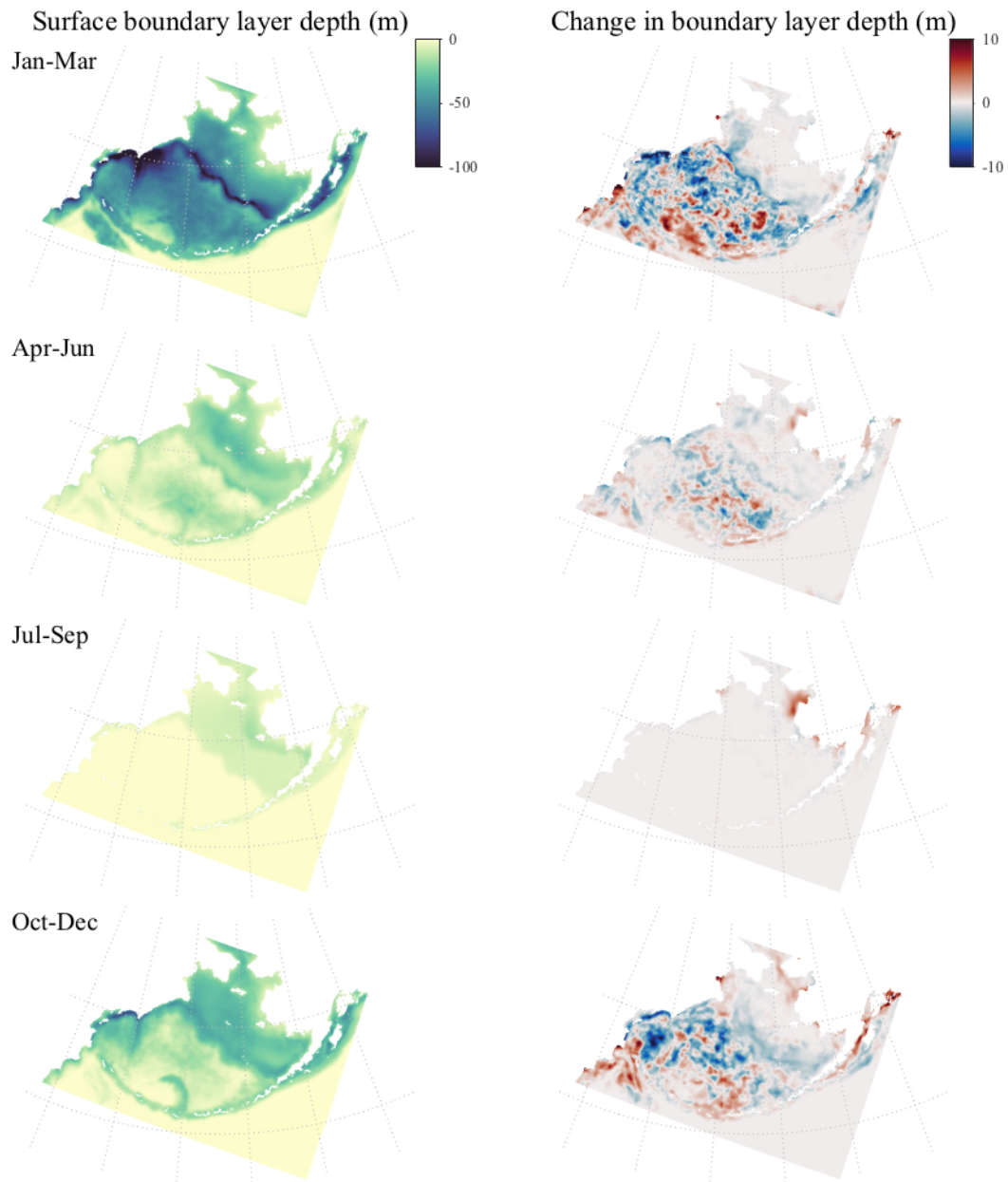


Figure 6. -- Surface boundary layer depth in the new-rivers simulation relative to the old-rivers simulation. Surface boundary layer depth represents the minimum Ekman depth in the model, and is used here as an approximation of mixed layer depth. A positive change indicates as shallowing of the mixed layer in the new-rivers simulation relative to the old-rivers simulation.

## CITATIONS

- Bodo, B. 2000. Russian River Flow Data by Bodo, Enhanced. URL <http://rda.ucar.edu/datasets/ds553.2/>. Accessed 10-18-2015.
- Dai, A. and K. E. Trenberth. 2002. Estimates of freshwater discharge from continents: Latitudinal and seasonal variations. *J. Hydrometeorol.* 3(6):660–687.
- Danielson, S., E. Curchitser, K. Hedstrom, T. Weingartner, and P. Stabeno. 2011. On ocean and sea ice modes of variability in the Bering Sea. *J. Geophys. Res. Ocean.* 116(June):1–24.
- Dean, K. G., C. McRoy, K. Ahlnäs, and A. Springer. 1989. The plume of the Yukon River in relation to the oceanography of the Bering Sea. *Remote Sens. Environ.* 28:75–84. URL <http://www.sciencedirect.com/science/article/pii/0034425789901065>.
- Fekete, B. M., C. J. Vörösmarty, and W. Grabs. 2002. High-resolution fields of global runoff combining observed river discharge and simulated water balances. *Glob. Biochem. Cycles* 16(3):15–1–15–6.
- Garcia, D. 2010. Robust smoothing of gridded data in one and higher dimensions with missing values. *Comput. Stat. Data Anal.* 54(4):1167–1178. URL <http://dx.doi.org/10.1016/j.csda.2009.09.020>.
- Hermann, A. J., G. A. Gibson, N. A. Bond, E. N. Curchitser, K. Hedstrom, W. Cheng, M. Wang, P. J. Stabeno, L. Eisner, and K. D. Cieciel. 2013. A multivariate analysis of observed and modeled biophysical variability on the Bering Sea shelf: Multidecadal hindcasts (1970–2009) and forecasts (2010–2040). *Deep. Sea. Res. Part II Top. Stud. Oceanogr.* 94:121–139.
- Kachel, N. B., G. L. Hunt, S. A. Salo, J. D. Schumacher, P. J. Stabeno, and T. E.

Whitledge. 2002. Characteristics and variability of the inner front of the southeastern Bering Sea. *Deep. Sea. Res. Part II Top. Stud. Oceanogr.* 49(26):5889–5909.

Large, W. G. and S. G. Yeager. 2009. The global climatology of an interannually varying air–sea flux data set. *Clim. Dyn.* 33(2):341–364.

United States Geological Survey. 2016. National Water Information System data available on the World Wide Web (USGS Water Data for the Nation). URL <http://waterdata.usgs.gov/nwis/>. Accessed 2016-12-09.

Watershed Boundary Dataset. 2017. Coordinated effort between the United States Department of Agriculture-Natural Resources Conservation Service (USDA-NRCS), the United States Geological Survey (USGS), and the Environmental Protection Agency (EPA). The Watershed Boundary Dataset (WBD) was created from a variety of sources from each state and aggregated into a standard national layer for use in strategic planning and accountability. URL <http://datagateway.nrcs.usda.gov>. Accessed 09-07-2017.

## APPENDIX: DETAILS OF INDIVIDUAL RIVER RECONSTRUCTIONS

In this appendix, we present the details underlying the construction of a streamflow time series for each of the rivers used in this report.

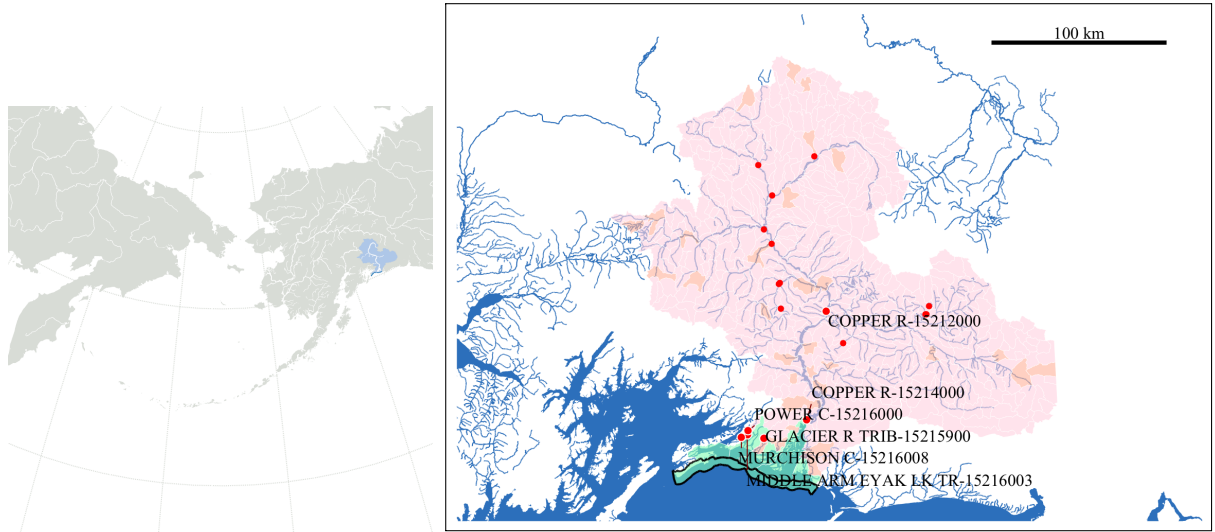
The period of time covered by each river measurement station varied widely from station to station; some provided daily coverage over several decades, while others were active for only a year or two. The vast majority of stations included gaps within their period of coverage, ranging from a few hours to several years. To build a complete monthly time series for each river between 1950 and 2016, we followed an iterative process:

1. The initial choice of stations to be used was based on a visual inspection of the discharge data available for each station on the river. We favored stations that were located close to the mouth of the river and that included as many years of data as possible.
2. If any gaps in time remained, we examined data from any remaining upstream measurement stations. We searched for stations that included data that overlapped in time with the downstream data at some point, as well as covering a portion of the gap in the downstream data. Using points in time shared between the two stations, we fit a shape-preserving spline between the upstream and downstream station streamflow values, and used that spline fit to estimate downstream flow from upstream values.
3. Using the daily time series from steps 1 and 2 (which may still include gaps), we averaged the resulting time series across 5-day bins (the 02/25-03/02 included 6 days during leap years). From the 5-day-averaged time series, we constructed a climatological single-year time series.
4. Where gaps remained in the 5-day-averaged time series, we filled in values from the climatological time series.
5. For any gaps that still remained (which were present if data from a station was only collected during certain times of year, leaving gaps in the climatological time series),

we filled in the time series using a smoothing spline (Garcia 2010).

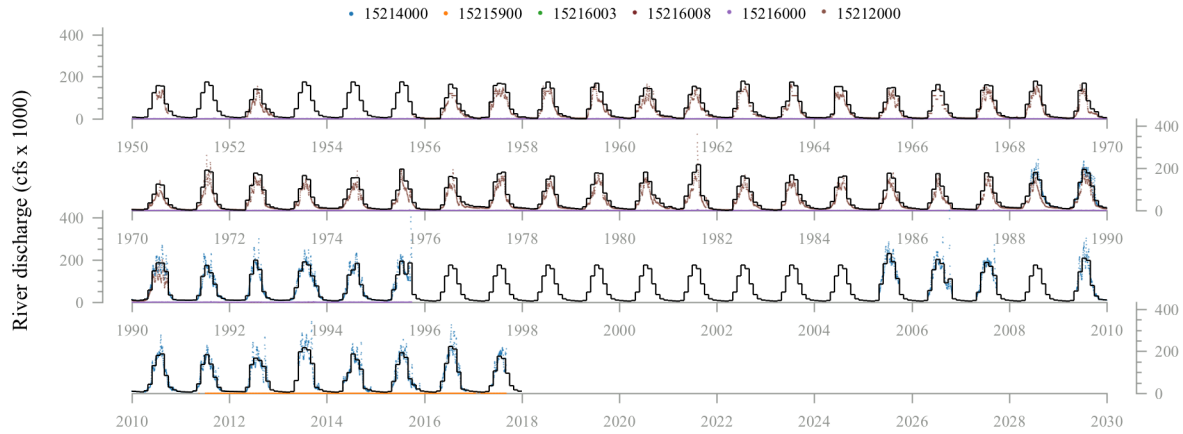
The following sections describe the locations of each of the watersheds, and detail the thought process behind choosing which stations to feed into the above method. All USGS monitoring stations are identified by their 8- to 15-digit site identification number. The detailed maps of each watershed (panel b of each figure) show the individual hydrographic units that make up each watershed, colored by classification: pink = standard, blue-green = frontal, orange = multiple, blue = water, and brown = island. All monitoring stations are shown as red dots, with labels applied only to those used in the final time series reconstructions. The time series panel (c) indicates daily values data from the gauging stations used in the final streamflow calculation as colored dots (colors are for contrast and do not indicate any particular property of each station), with the sum total streamflow for the watershed indicated as a black line.

# Hook Point-Frontal Gulf of Alaska



(a) Watershed location

(b) Hydrologic units and station locations.



(c) Time series

Figure A.1. -- Streamflow to this location is dominated by the Copper River. We used station 15214000 as the primary source, with 15212000 scaled to fill in earlier years. Eyak Lake Tributary, Murchison Creek, and Glacier River Tributary have one site each, which were added to the total.

# Resurrection Bay-Frontal Gulf of Alaska

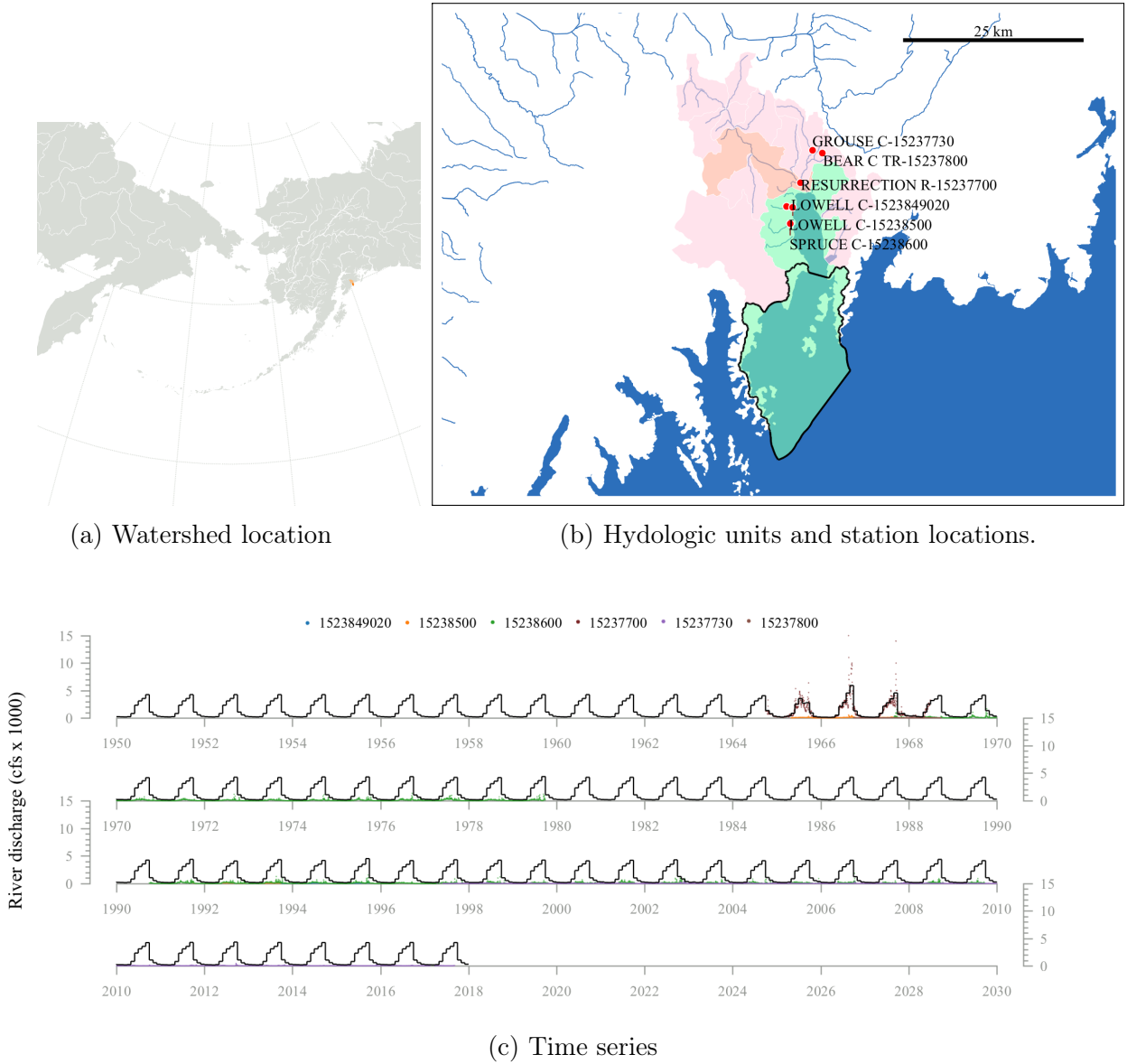
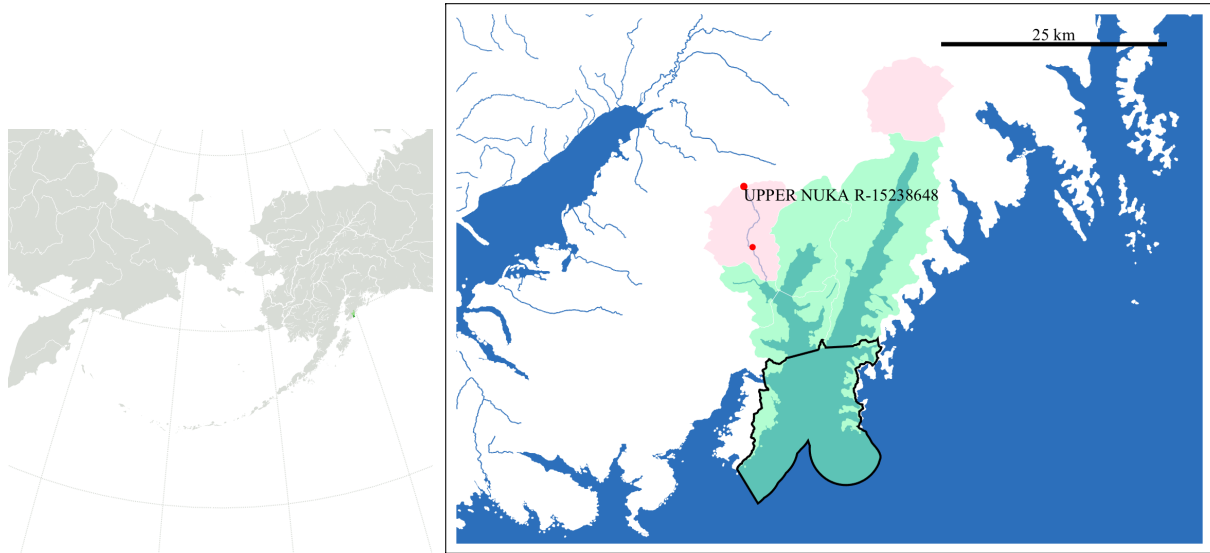


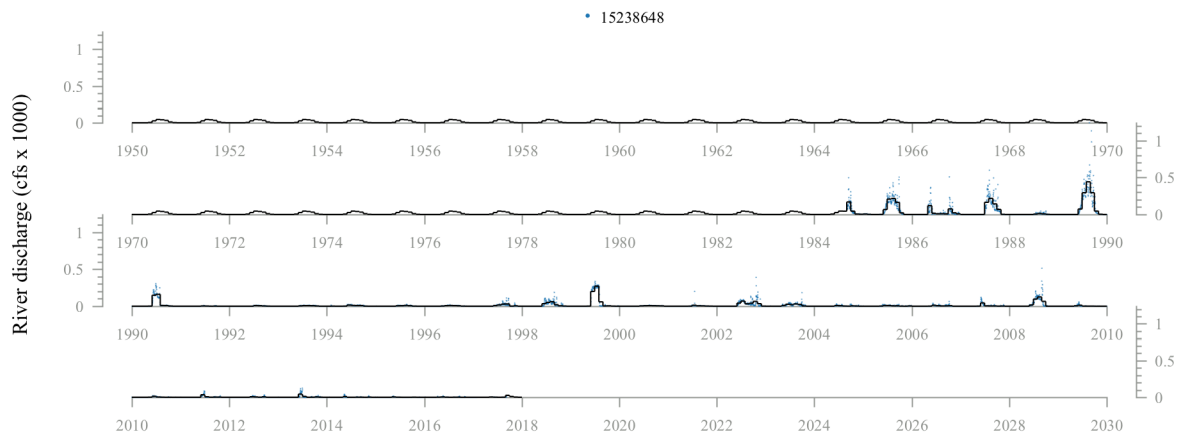
Figure A.2. -- Lowell Creek included two stations with comparable measurements and no time overlap; this data was combined without scaling. All other rivers used the singular station available. Total discharge to this watershed primarily reflects the flow from Resurrection River.

# Nuka Bay-Frontal Gulf of Alaska



(a) Watershed location

(b) Hydrologic units and station locations.



(c) Time series

Figure A.3. -- The downstream station for the Nuka River was active for only one year, so we opted to use the more recent, longer running upstream station for this small watershed.

# Prince William Sound

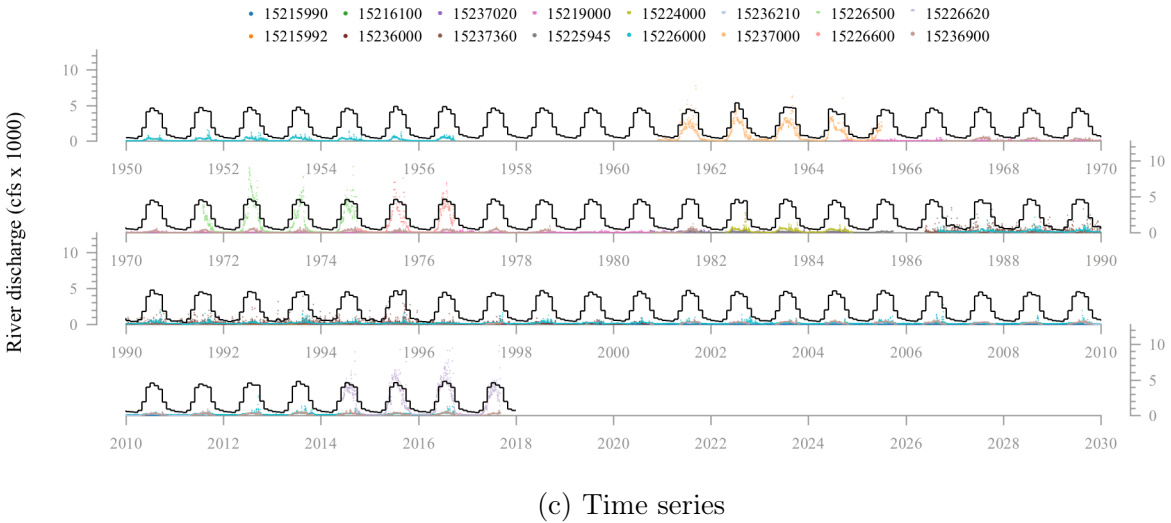
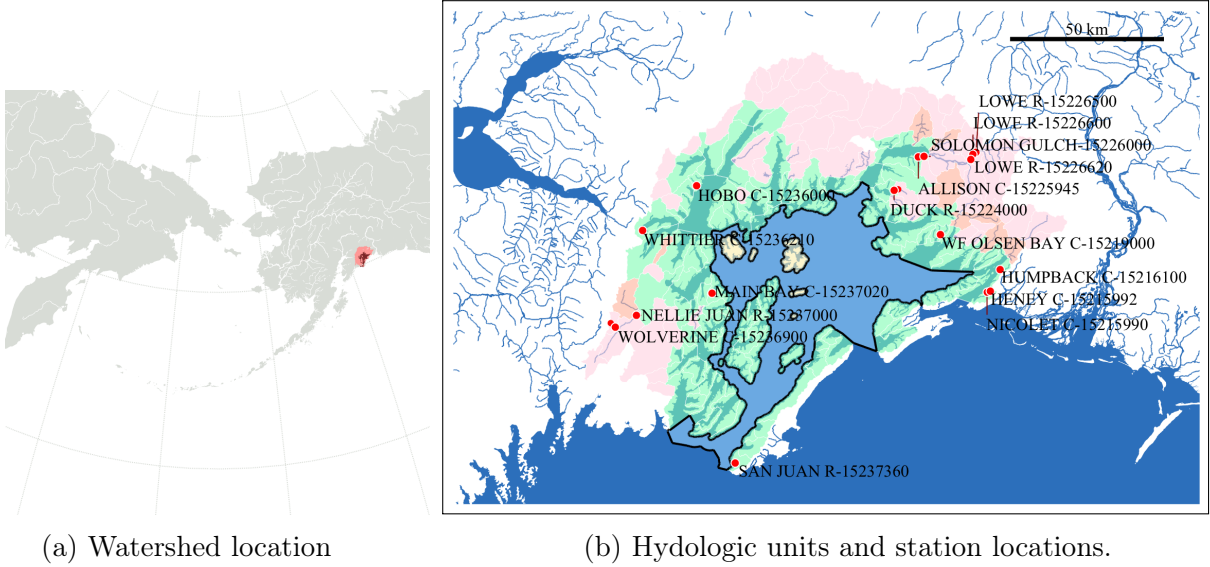
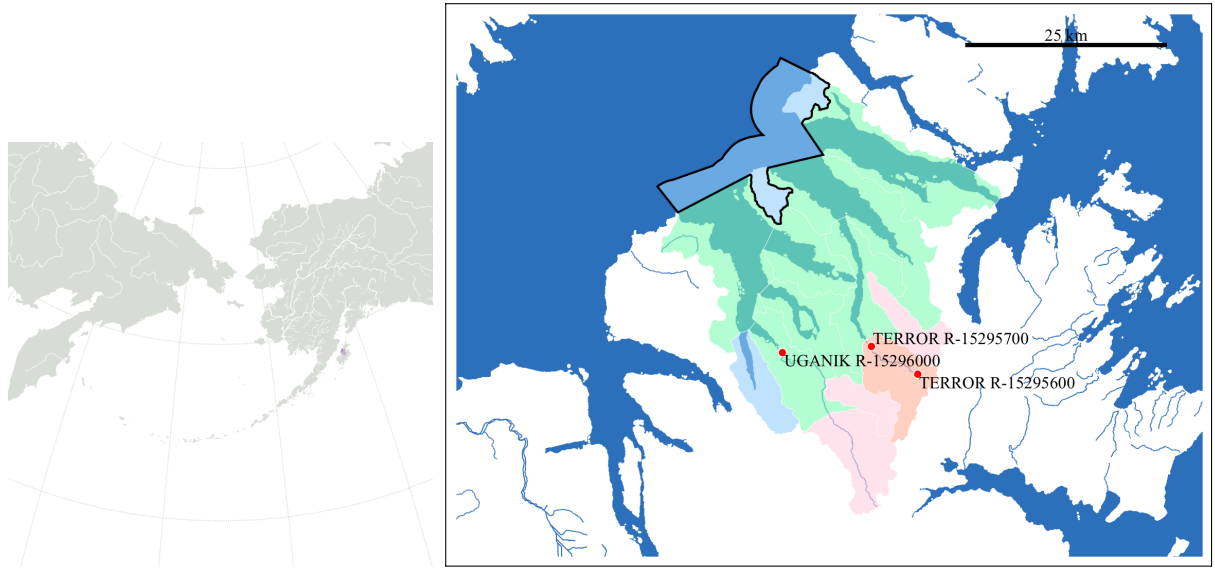


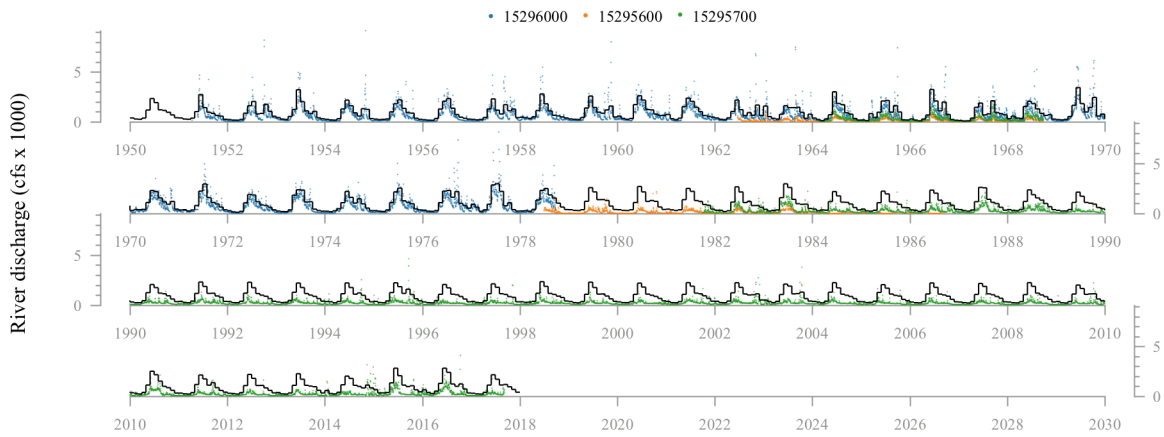
Figure A.4. -- Prince William Sound receives discharge from many river and creeks, several of which included multiple stream gauges. The two stations on Solomon Gulch overlap for most of their coverage; we chose to use 15226000 because it covered a longer timeperiod. The Lowe River included three stations, all with comparable discharge magnitudes and with no temporal overlap, so we combined these into a single time-series. The Duck River stations overlapped in time; 15224000 was chosen due to its downstream location. The remaining rivers included one station each that could be added to the total discharge value.

# Cape Uganik-Shelikof Strait



(a) Watershed location

(b) Hydrologic units and station locations.



(c) Time series

Figure A.5. -- The Cape Uganik watershed includes two small rivers of comparable size. We primarily used station 15295700 for the Terror River, with a scaled version of 15296000 added to fill gaps in the earlier part of the timeseries. This was added to the Uganik River to get a total discharge for the watershed.

## Sevenmile Beach-Frontal Shelikof Strait

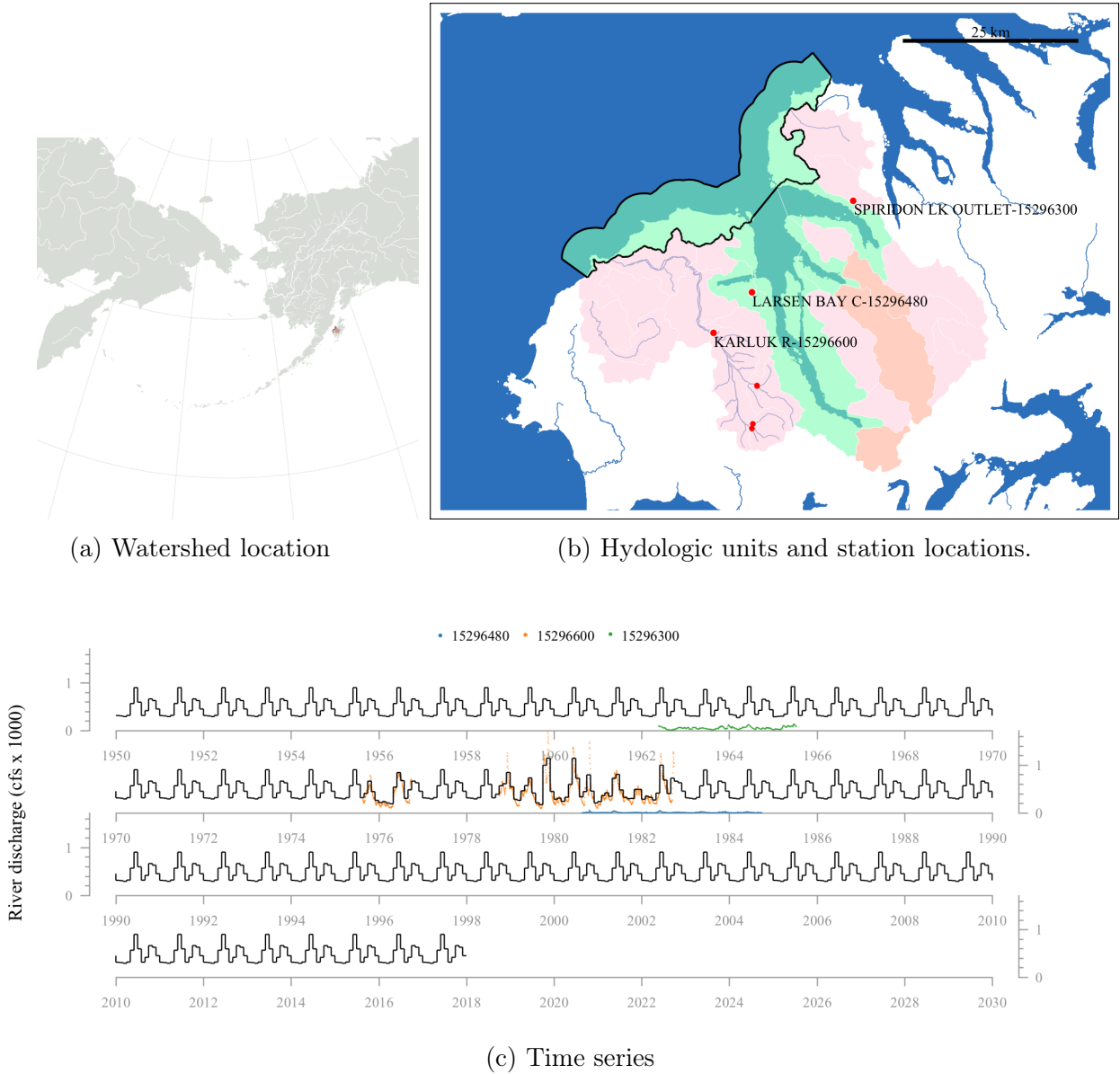
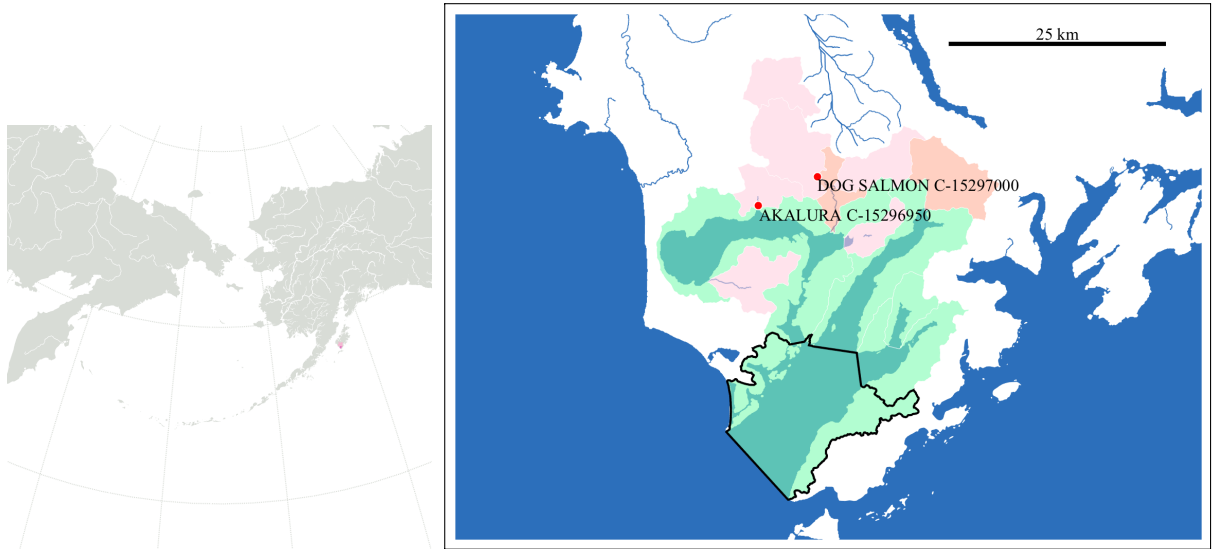


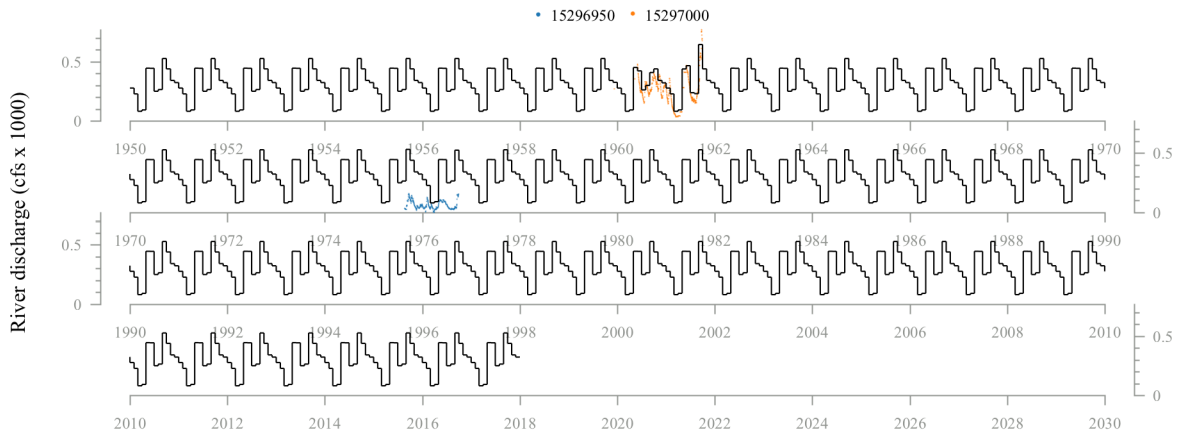
Figure A.6. -- This small watershed on Kodiak Island includes only a few short time-series. We chose the most downstream station from the Karluk River and added data from two other small creeks.

# Alitak Bay-Frontal Pacific Ocean



(a) Watershed location

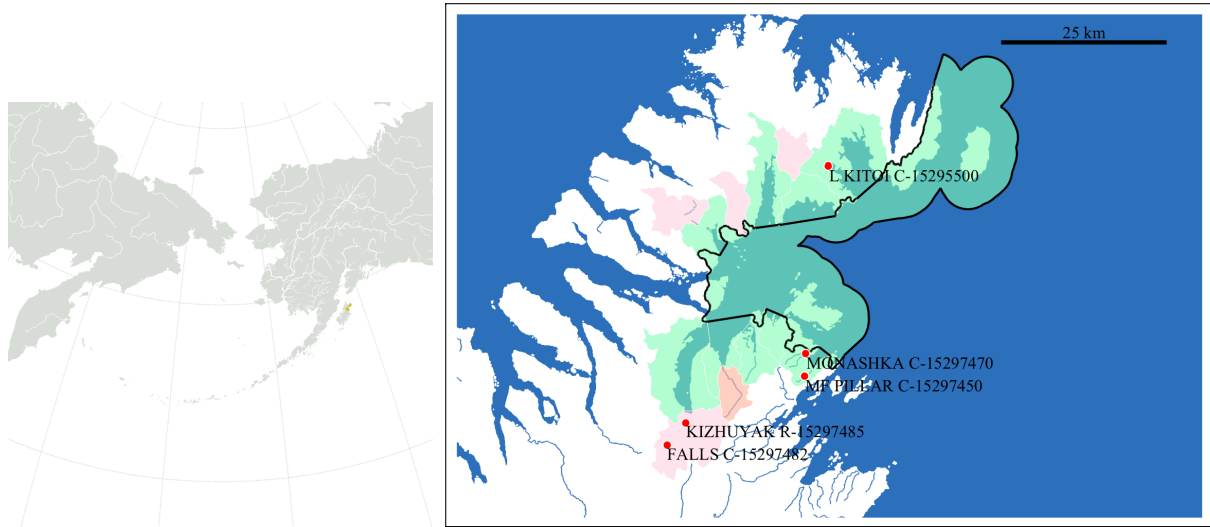
(b) Hydrologic units and station locations.



(c) Time series

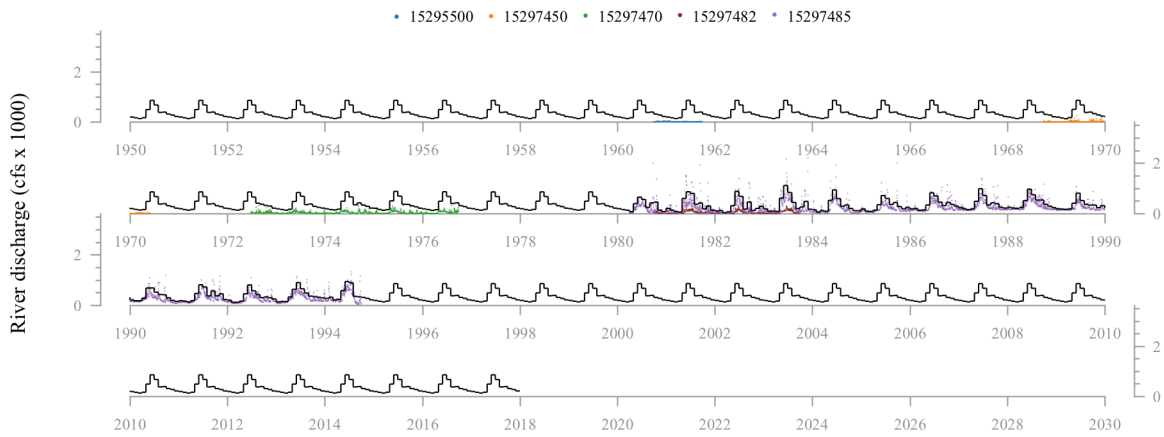
Figure A.7. -- The southern tip of Kodiak island is also sparsely monitored, with only two short-lived gauges located in this watershed. Both stations' data were added together to create this timeseries.

# Tonki Cape Peninsula-Frontal Marmot Bay



(a) Watershed location

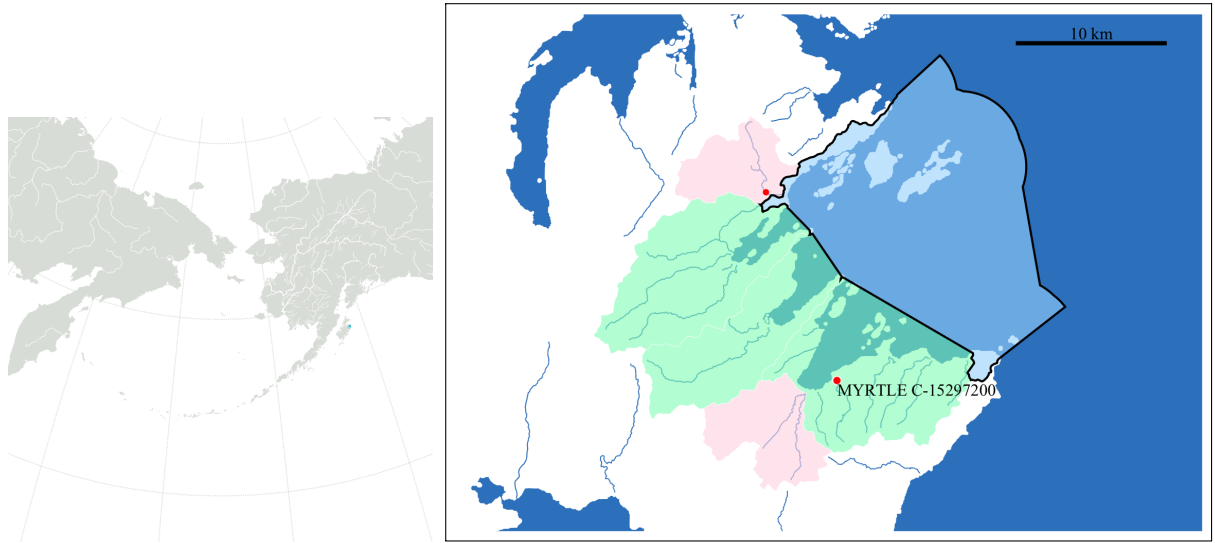
(b) Hydrologic units and station locations.



(c) Time series

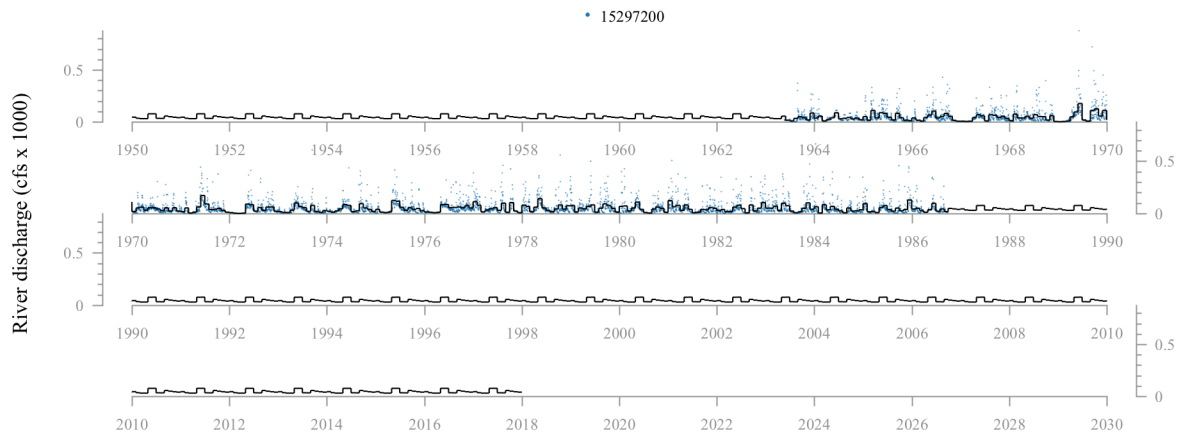
Figure A.8. -- Each river in this watershed included a single station, so all data sources were used in the timeseries.

# Chiniak Bay



(a) Watershed location

(b) Hydrologic units and station locations.



(c) Time series

Figure A.9. -- The Buskin River station included only a few days worth of discharge data, so we opted to use only the Myrtle Creek timeseries for this watershed.

## Sacramento River-Frontal Pacific Ocean

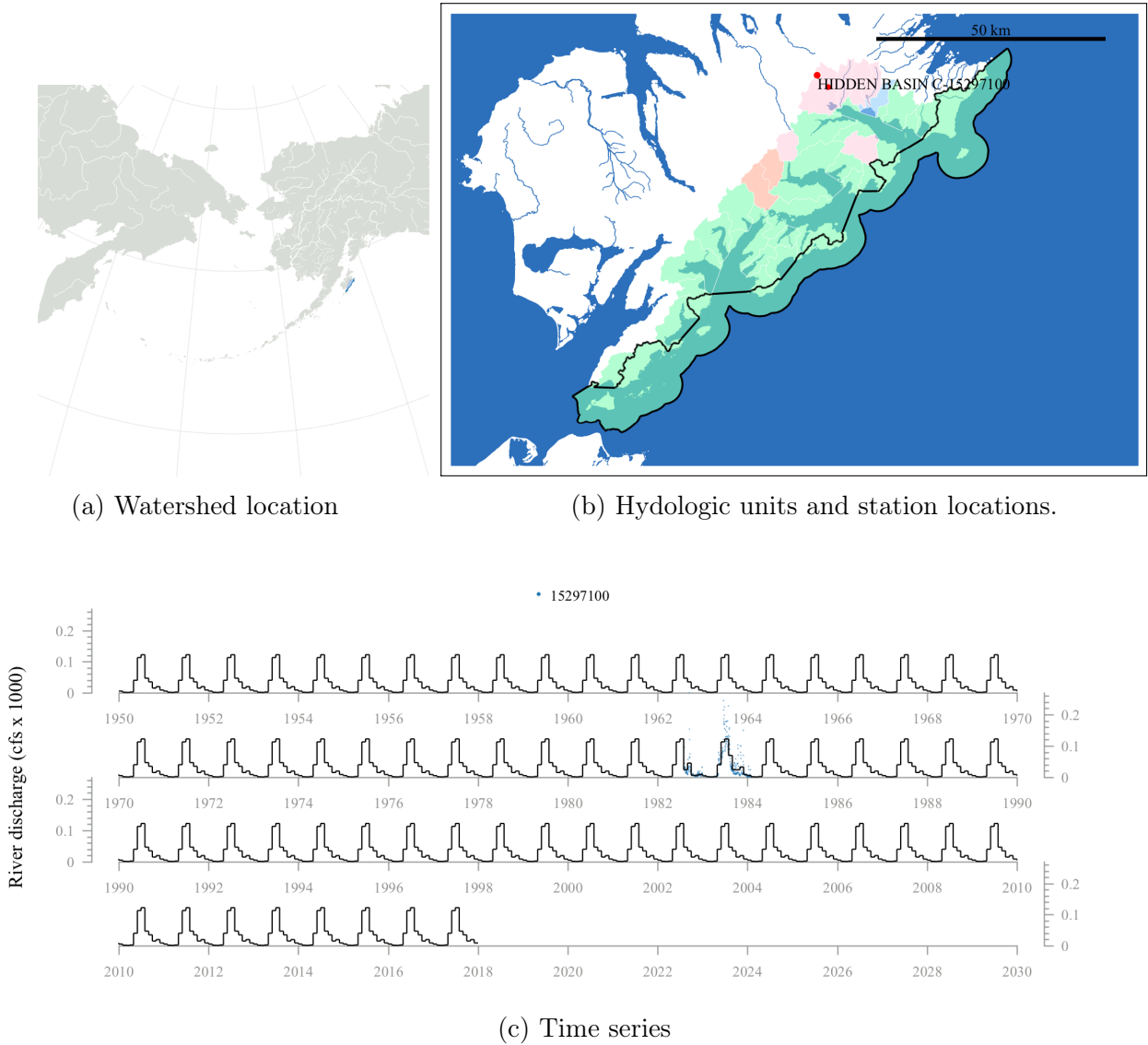


Figure A.10. -- Both stations in this watershed are located on Hidden Creek, and both cover the same short period of time. We opted to use the more downstream of these two stations to represent the watershed.

# Sutwik Island-Pacific Ocean

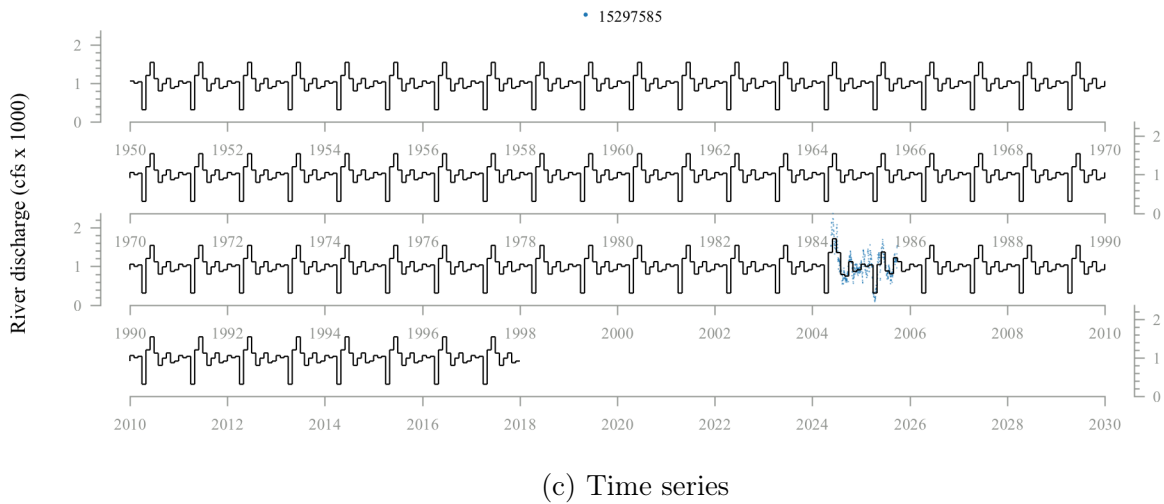
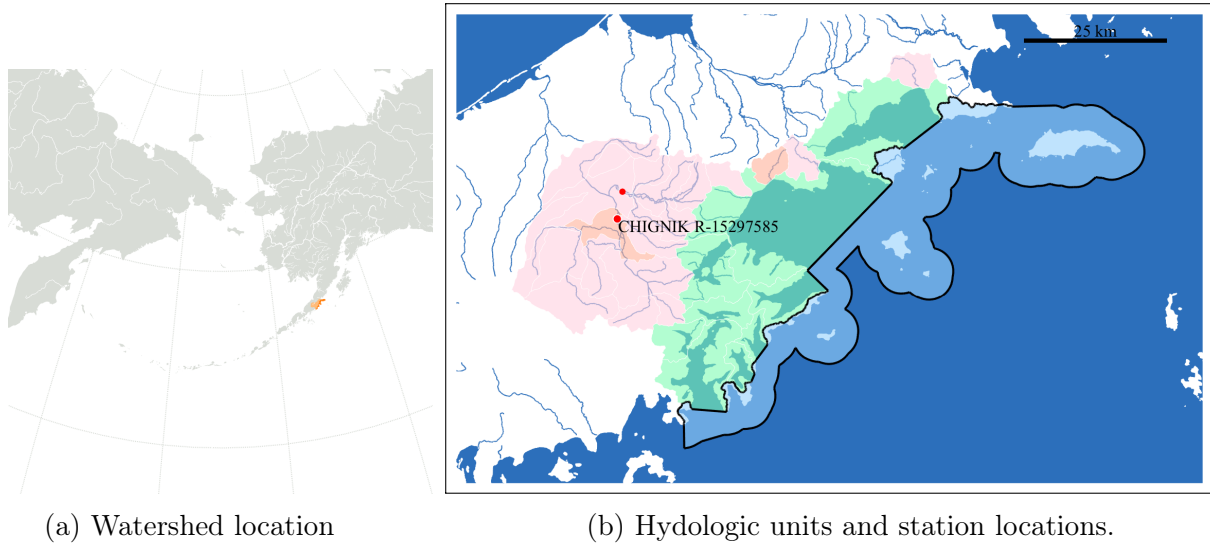


Figure A.11. -- Only two stations are available for this watershed; the Alec River is a tributary of the Chignik River, so we used only data from the latter.

# Cook Inlet

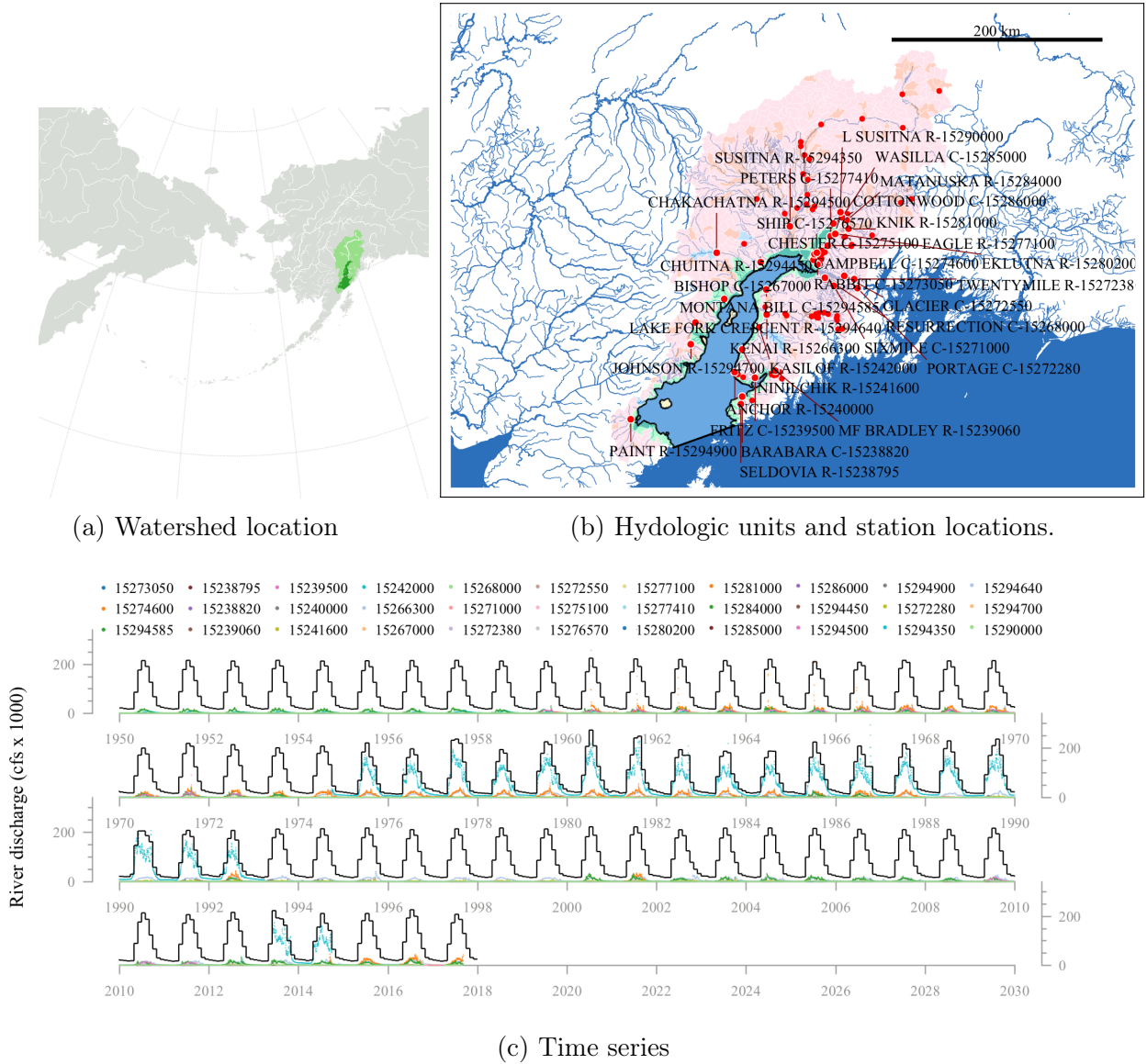


Figure A.12. -- Cook Inlet receives input from dozens of rivers, including several of the largest in our study; the Knik, Kenai, Matanuska, and Chakachatna Rivers all average over 5000 ft<sup>3</sup>/s, and the Susitna averages over 50000 ft<sup>3</sup>/s. Because the Susitna River dominates the total streamflow, we did not bother looking for scalable upstream stations in this watershed, but simply chose the most downstream location available for each of the 33 gauged tributaries.

## Unga Island-Frontal Pacific Ocean

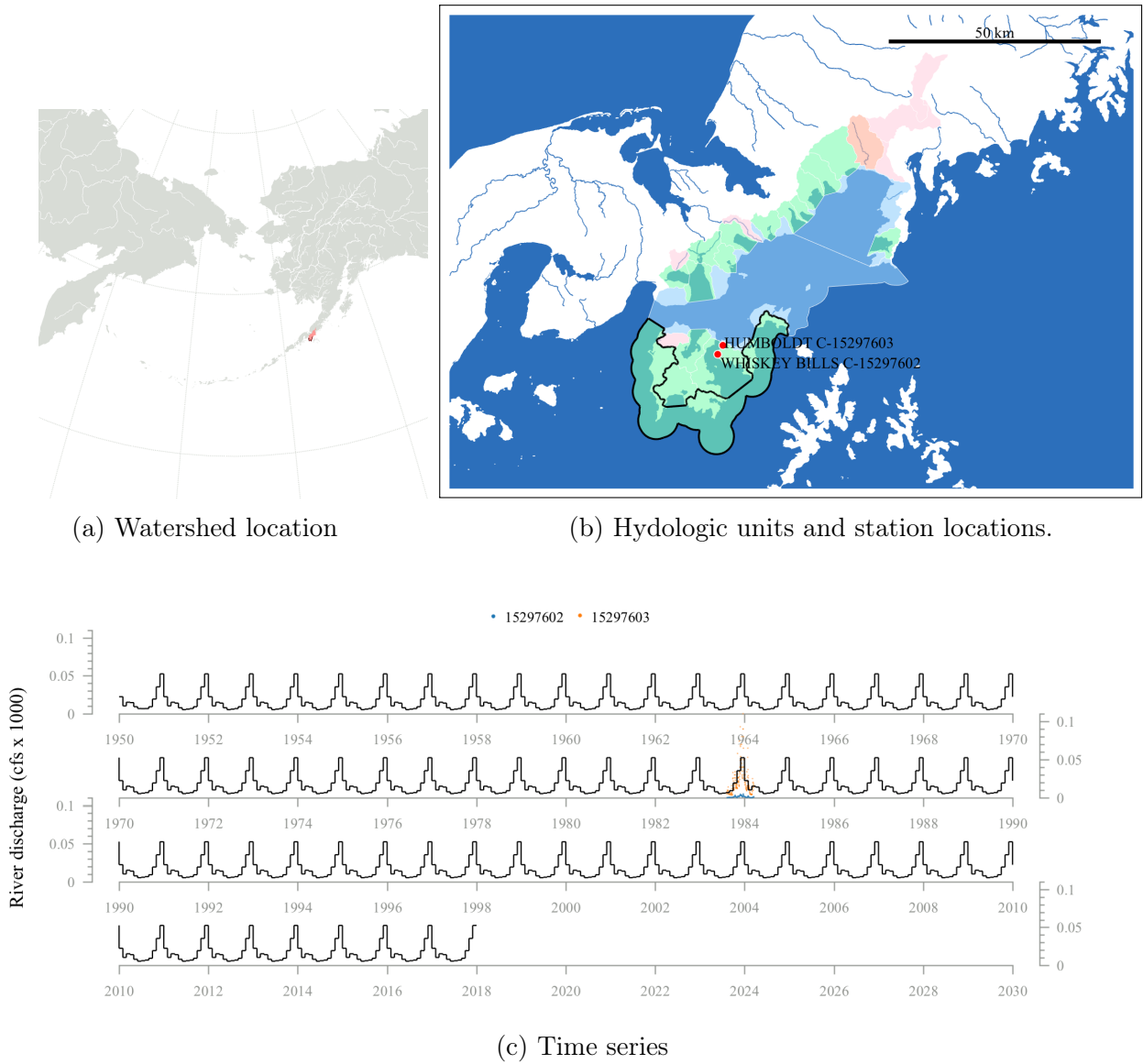
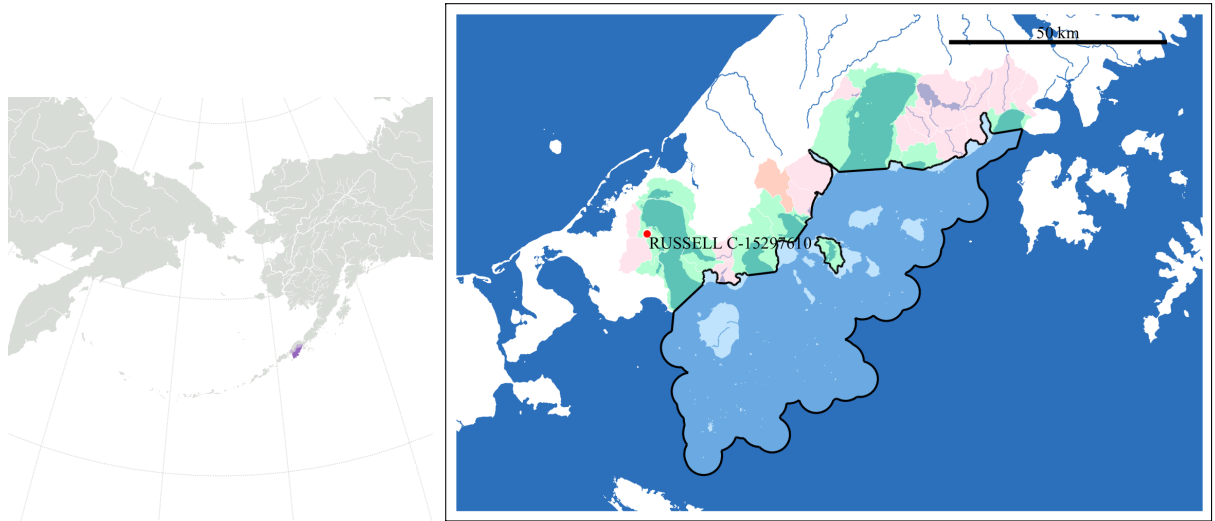


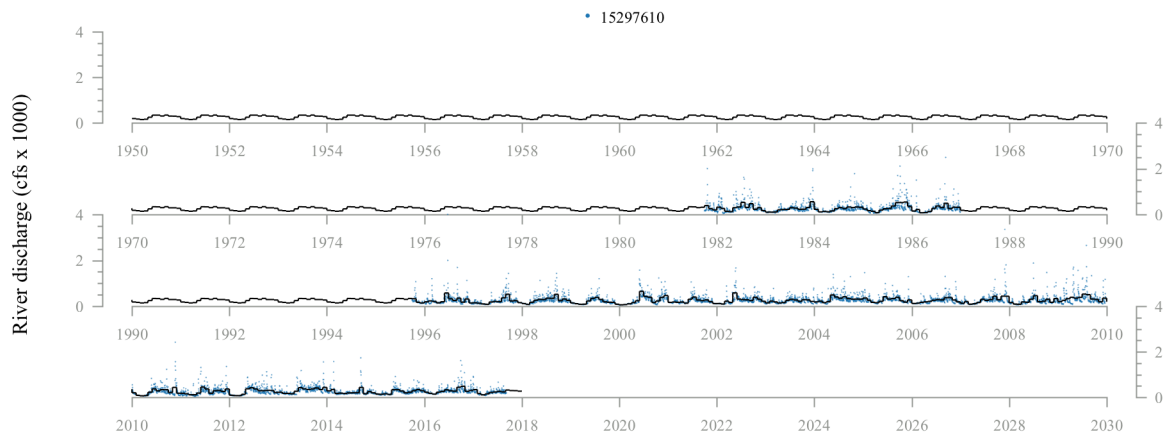
Figure A.13. -- Only two small creeks are monitored in this watershed, and both include only a single year of data. These were added together for the total discharge.

# Deer Island



(a) Watershed location

(b) Hydrologic units and station locations.



(c) Time series

Figure A.14. -- Russel Creek is the only monitored creek in this watershed, and therefore was used alone to represent this location.

190301030000

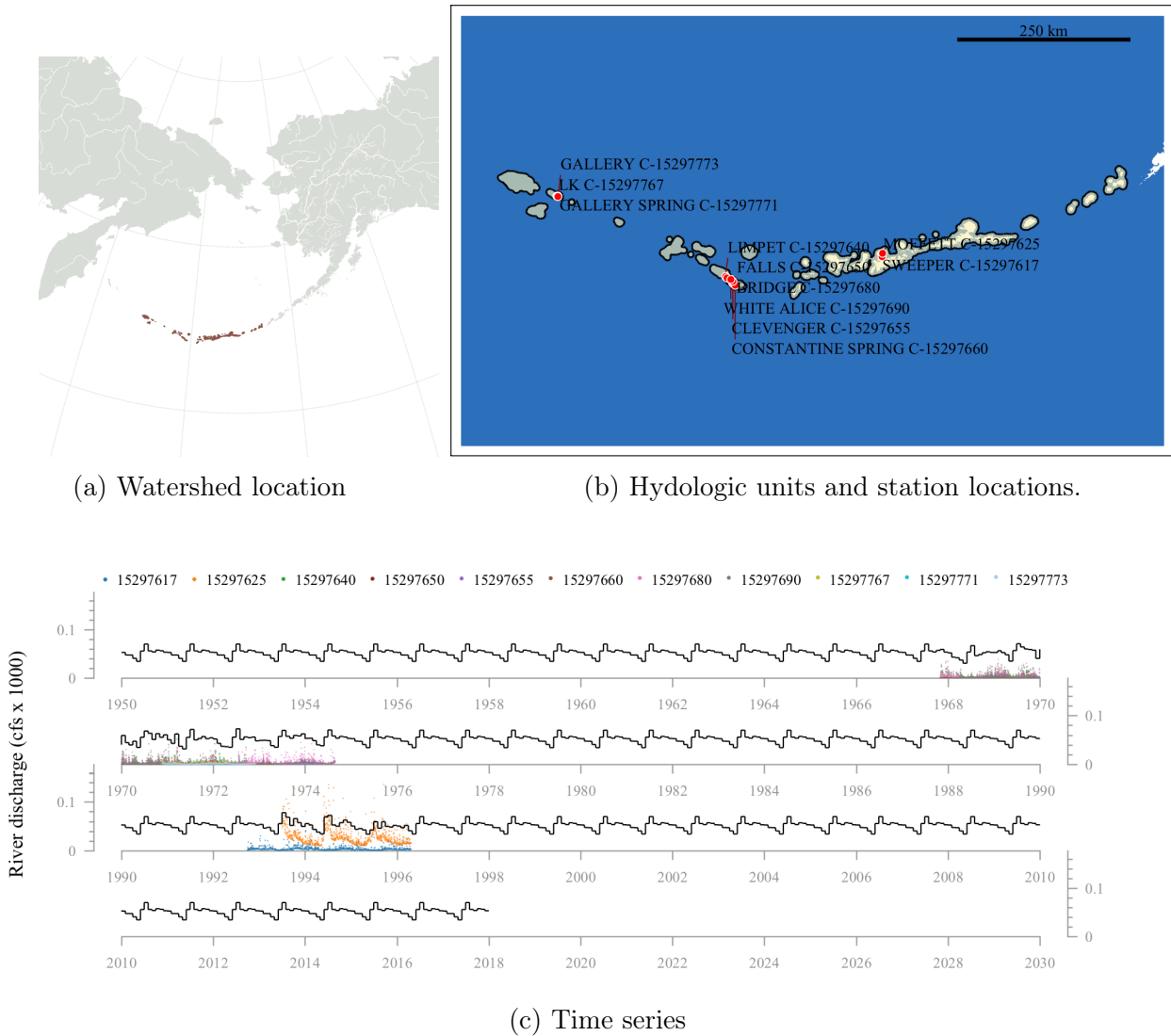


Figure A.15. -- The eastern Aleutian Islands are represented by a single hydrological unit. Stream gauges are located on three of the islands: Adak, Amchitka, and Shemya Islands. We opted to simply sum together values from all gauges in the watershed and distribute the flow as though it were evenly distributed throughout the island hydrologic unit. The streamflow in this region is several orders of magnitude lower than that seen from the largest rivers in our study area, and therefore we decided this assumption (as opposed to trying to distribute the streamflow proportionally to individual islands) has a negligible effect on our model results.

## Kvichack Bay-Frontal Bristol Bay

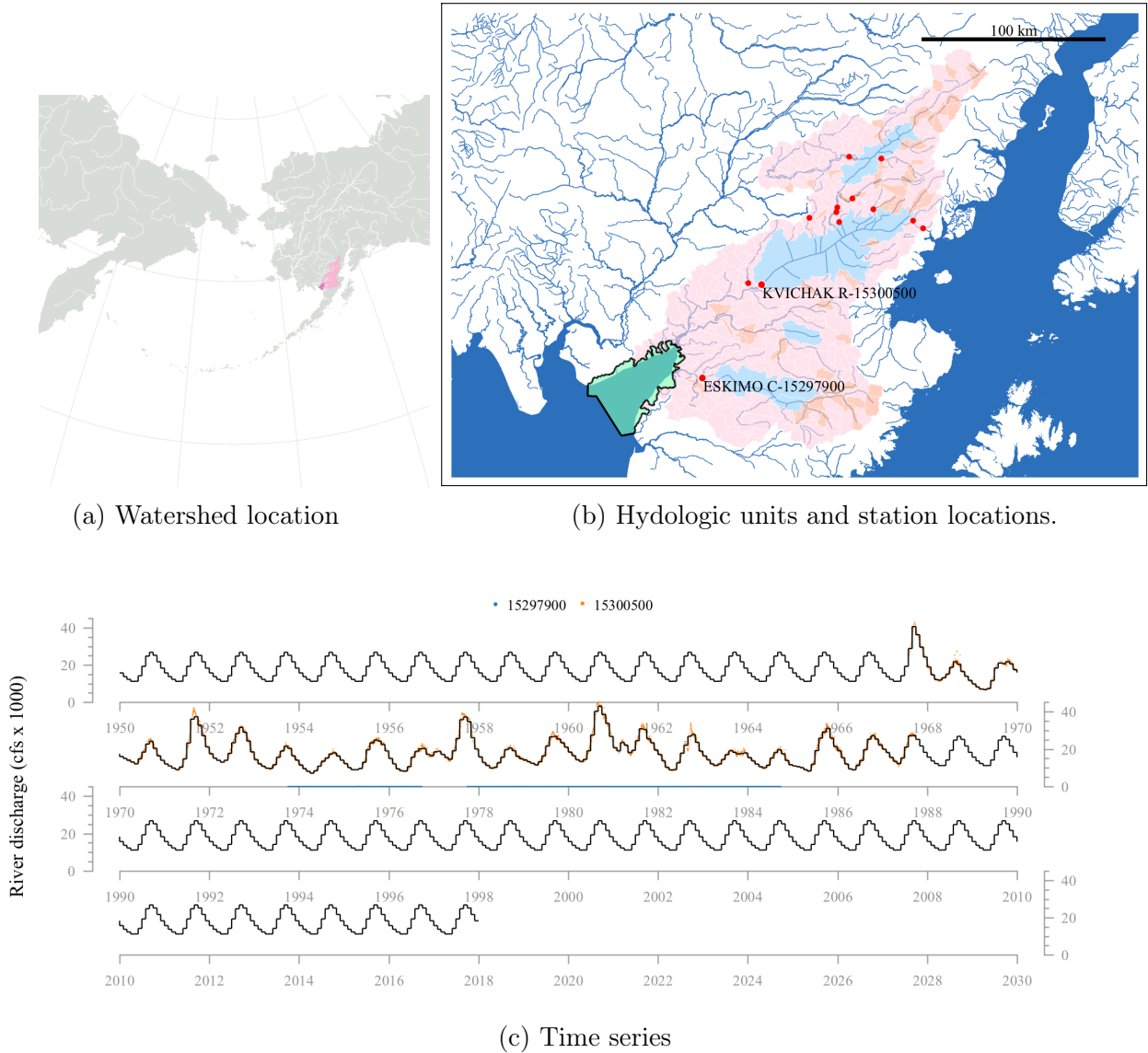


Figure A.16. -- The majority of the stations in this watershed are associated with the Kvichack River and tributaries of Lake Iliamna, where the Kvichack River originates. We used station 15300500, the only station located below Lake Iliamna, to represent that river system, and also added in data from Eskimo Creek.

## 190303060902-Frontal Nushagak Bay

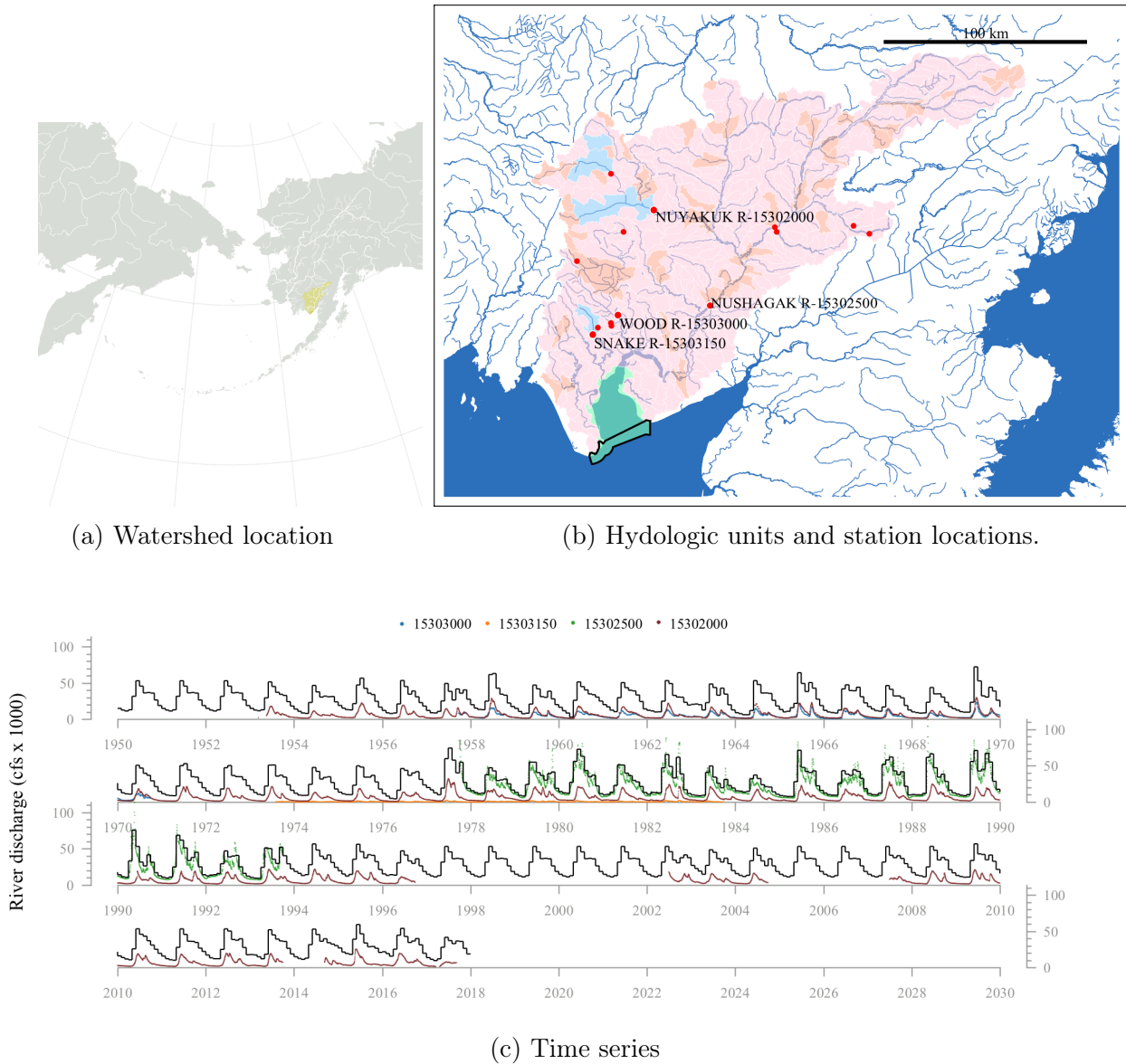
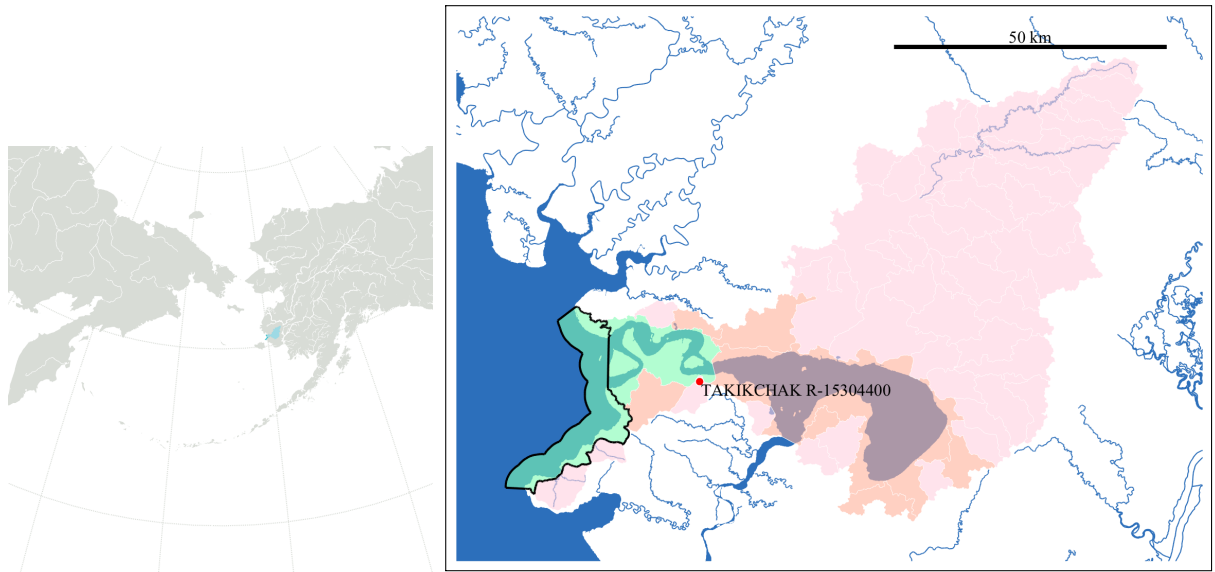


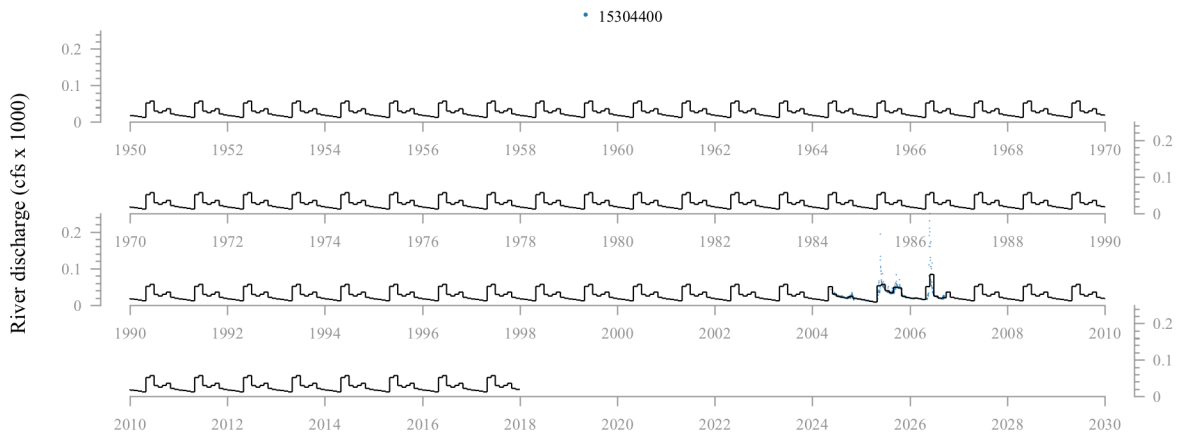
Figure A.17. — Three rivers in this system empty directly into Nushagak Bay: the Nushagak River, Wood River, and Snake River. The latter two of these were each represented by a single station. For the Nushagak, a long timeseries was available for one of its main tributaries, the Nuyayuk Ruver, so we scaled this data to extend the Nushagak timeseries. The three rivers were then added together to create the final timeseries.

# Ugchirnak Mountain-Frontal Hazen Bay



(a) Watershed location

(b) Hydrologic units and station locations.



(c) Time series

Figure A.18. -- This watershed is sparsely monitored, with only a single station with about two years' worth of data.

## Warehouse Bluff-Frontal Kuskokwim Bay

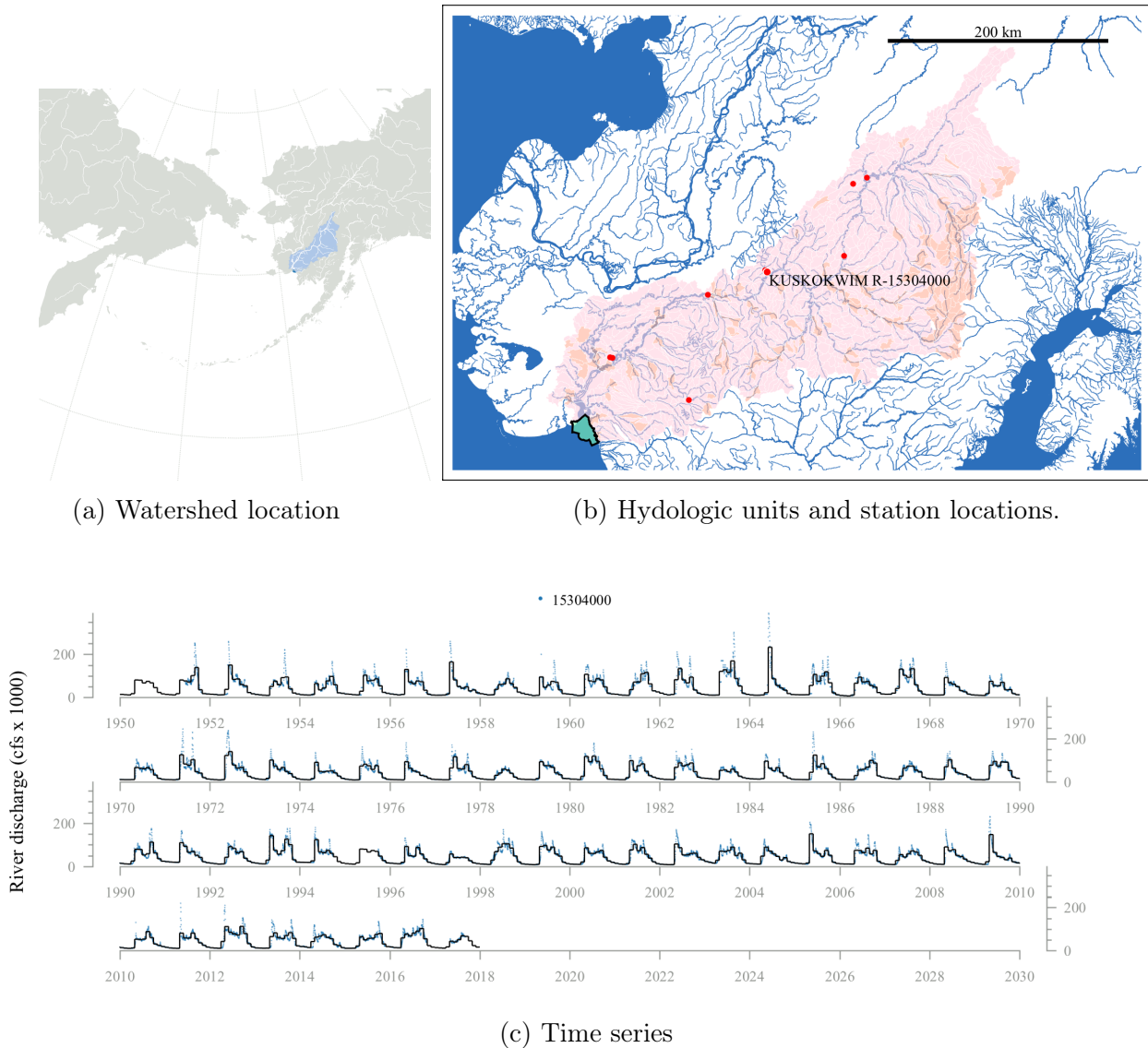


Figure A.19. -- All stations in this watershed are located along the Kuskokwim River and its tributaries. The station near Crooked Creek (15304000) has the most complete record, covering nearly the entirety of our timeperiod of interest. There are a few tributaries that feed into the river downstream of this point, but their additional streamflow is very small compared to that of the Kuskokwim upstream of that point. Therefore, we used the single station to represent this location.

# Taket Creek-Frontal Norton Sound

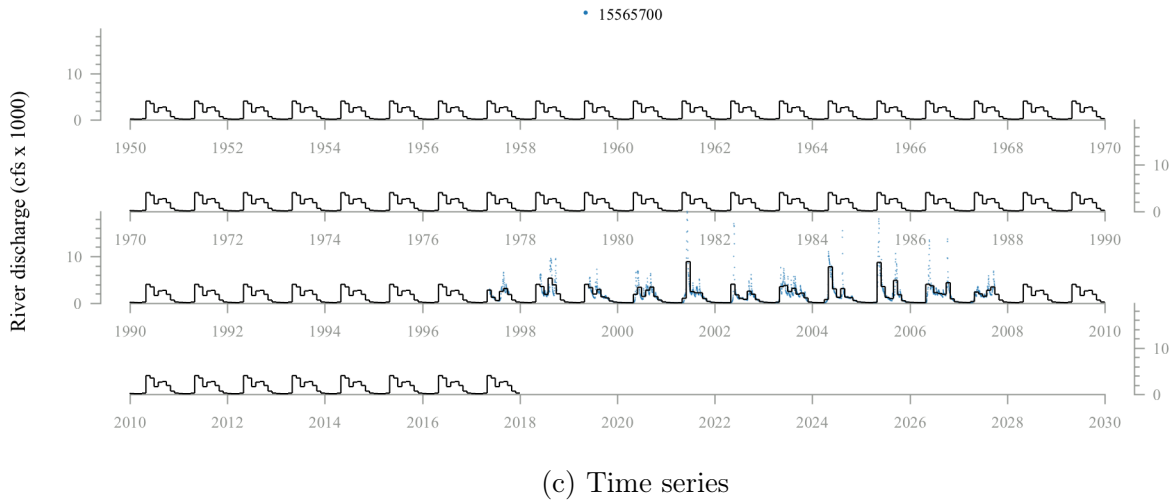
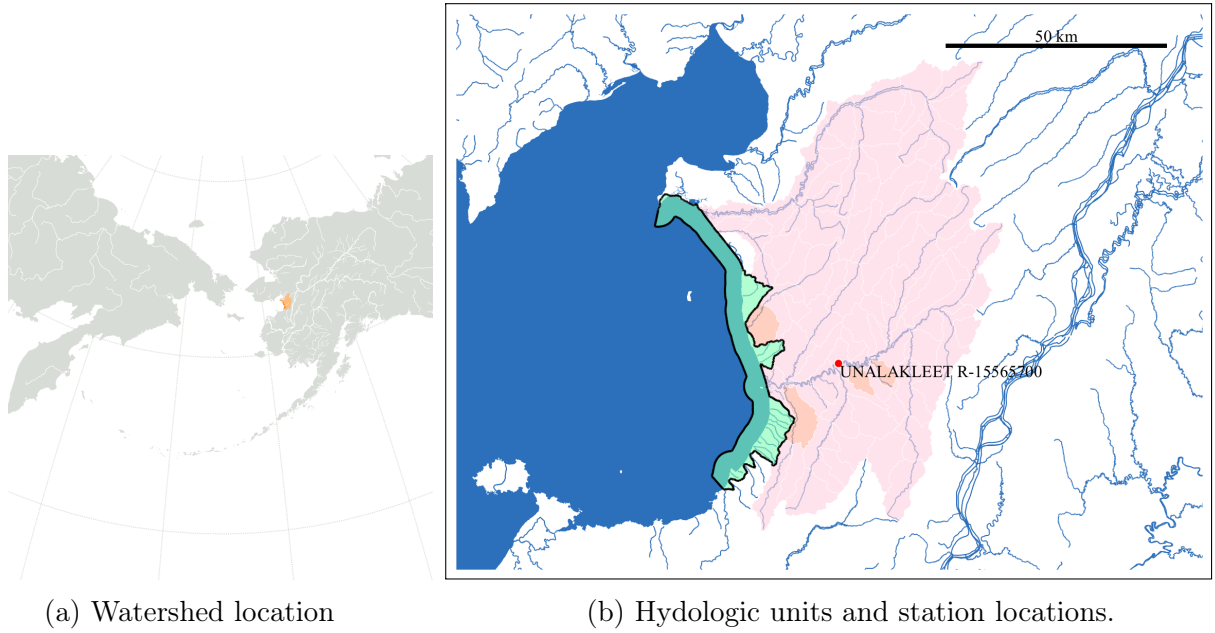
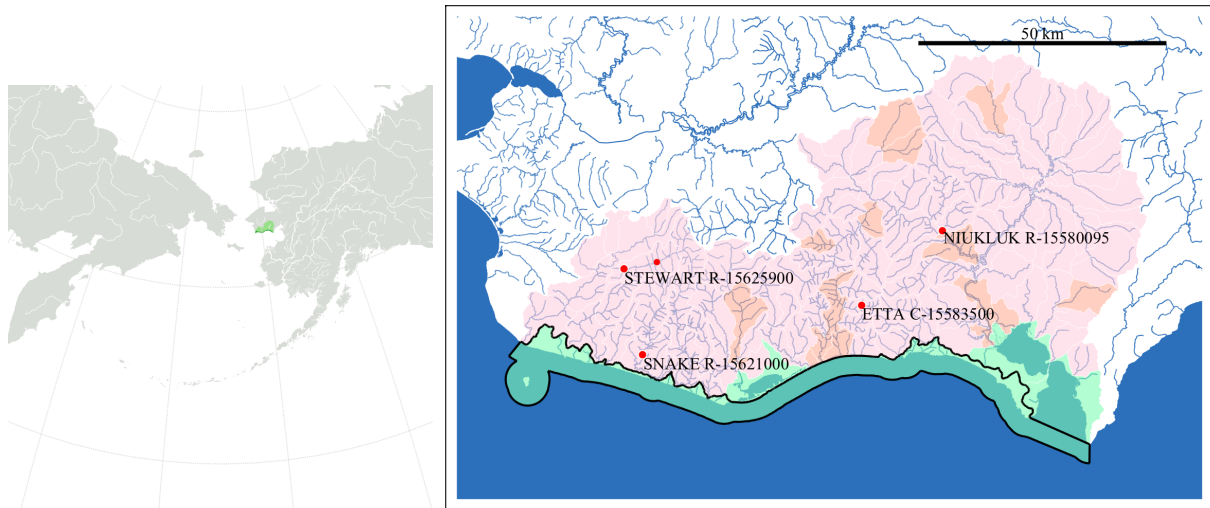


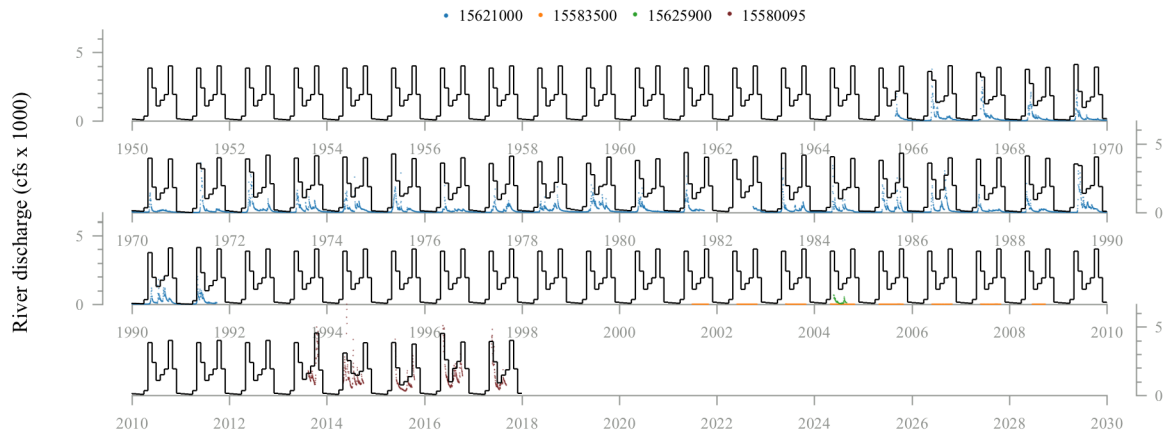
Figure A.20. -- Only the Unalakleet River included a gauge, so we used the data from this location to represent southern Norton Sound.

## Quartz Creek-Frontal Norton Sound



(a) Watershed location

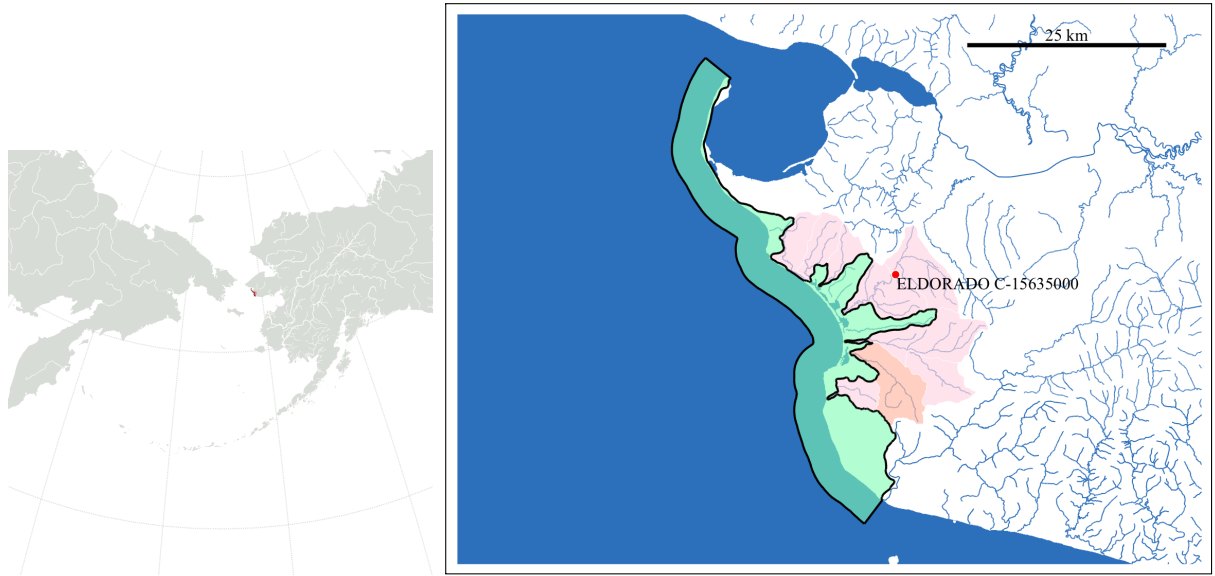
(b) Hydrologic units and station locations.



(c) Time series

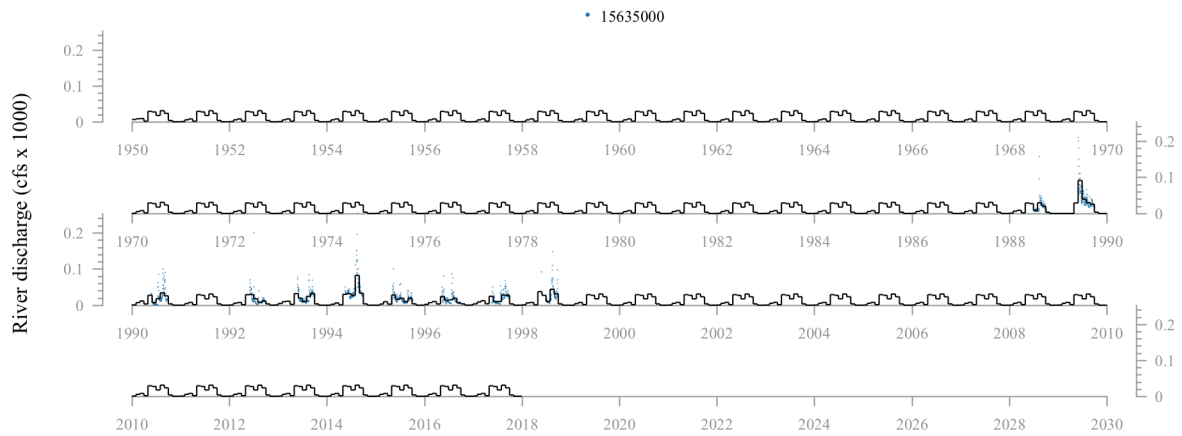
Figure A.21. -- Two stations were available for Stewart River; we chose to use the more downstream of these two. The remainder of the stations represented a single river each, and we added to the total streamflow for the watershed.

# Crete Creek-Frontal Bering Sea



(a) Watershed location

(b) Hydrologic units and station locations.



(c) Time series

Figure A.22. -- Only El Dorado Creek includes a monitoring station, so it was used to represent this watershed.

# King River-Frontal Bering Sea

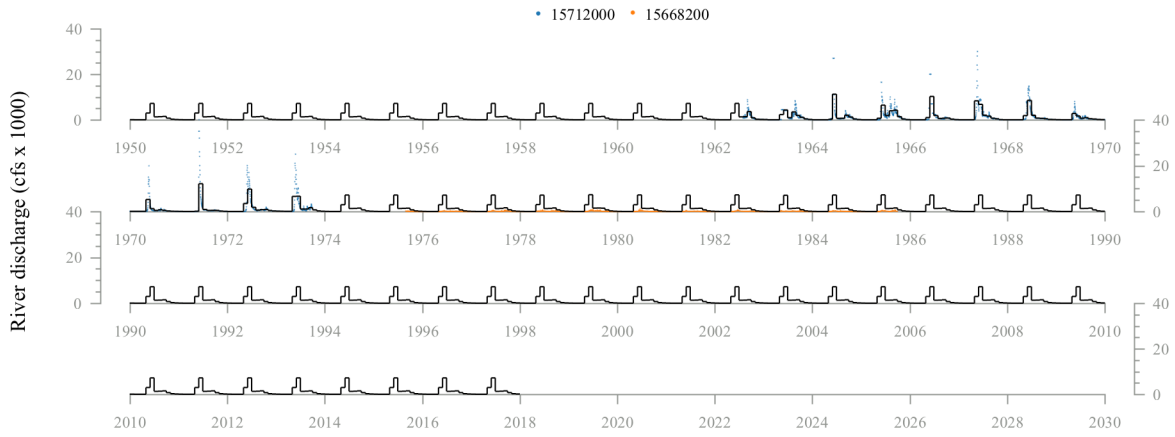
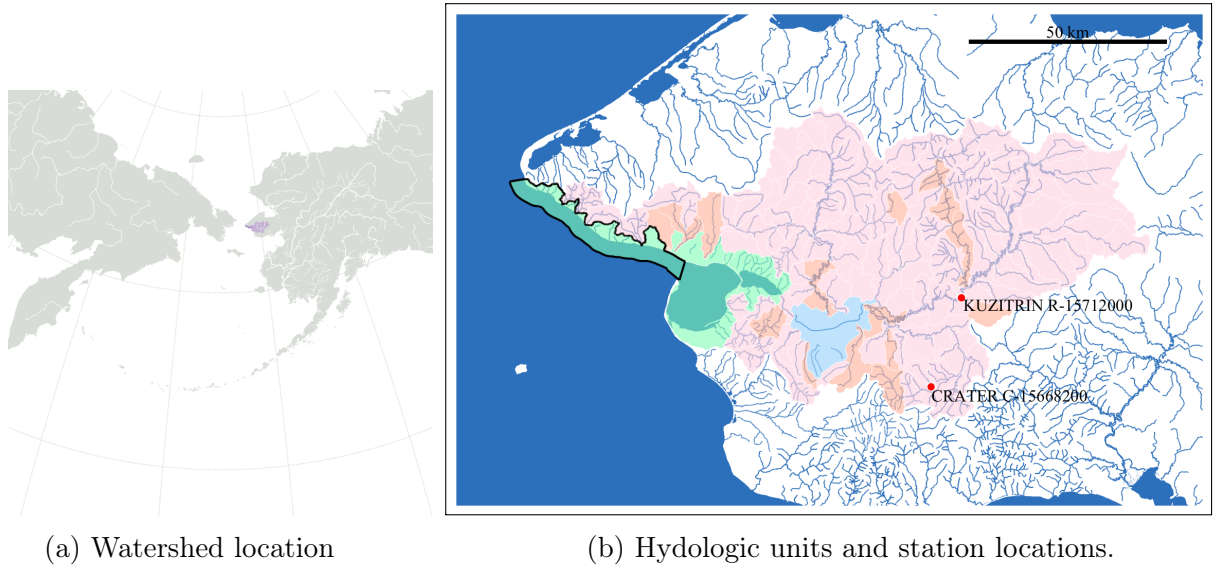


Figure A.23. -- Both stations available in this watershed are located above the Imuruk Basin, which receives most of the drainage from this region. However, lacking any downstream stations, these two were added together to get a streamflow for this watershed.

# Kotzebue Sound

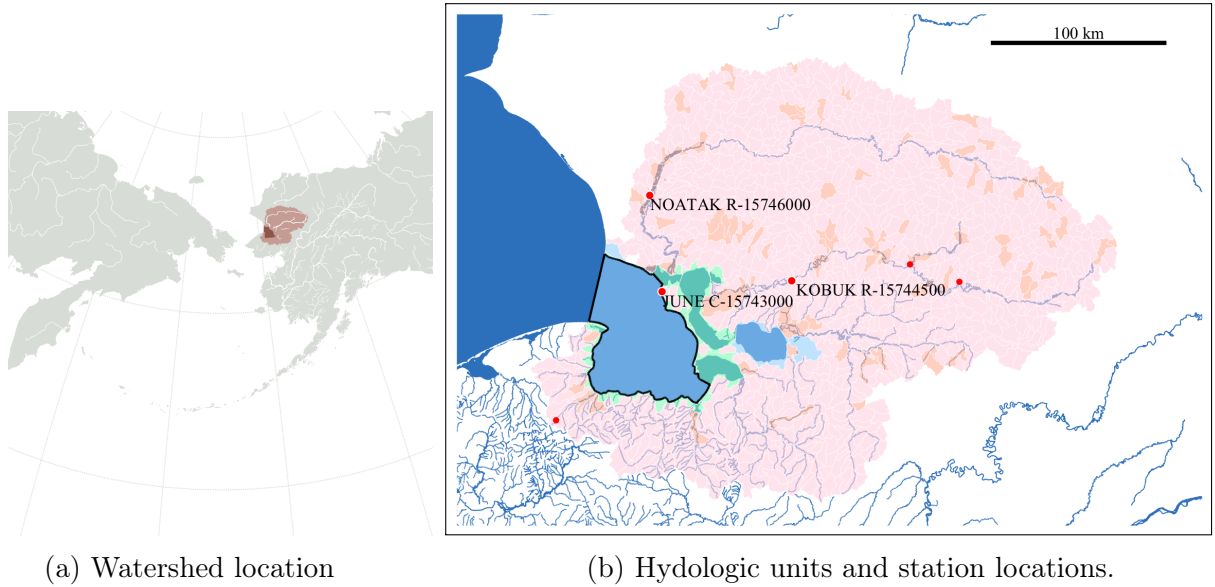


Figure A.24. -- The Noatak and Kobuk rivers dominate the streamflow at this location. The former included only one station, and for the latter we chose the most downstream station available. We also considered data from the smaller June and Humbolt Creeks; June Creek was added to the final total, but Humbolt was removed due to lack of sufficient data (less than one year).

## Outlet Yukon River-Frontal Bering Sea

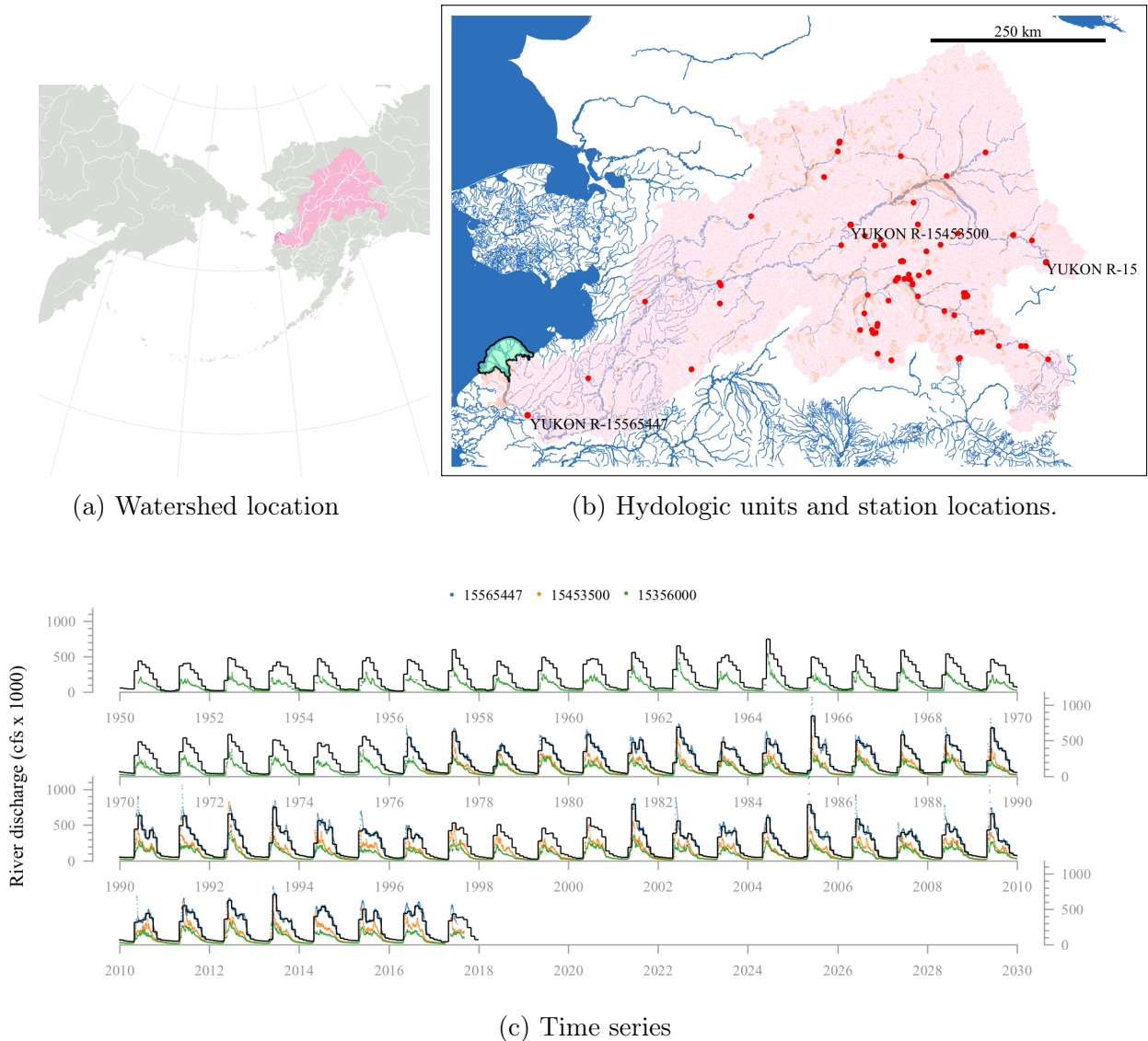


Figure A.25. -- This watershed encompasses the Yukon River drainage basin, the largest in the domain, both in area covered and total streamflow. Three stations were used to construct the total timeseries for this river. Station 15565447 is located closest to the mouth, and its data was used as is. Data from 15453500, the next closest to the river mouth, was scaled to the downstream station and used to fill a gap in the 90s. Finally, station 15356000, which included the most complete temporal record but is located far upstream, was scaled to the most downstream station and used to fill in the earlier part of the timeperiod of interest.

# Kamchatka River

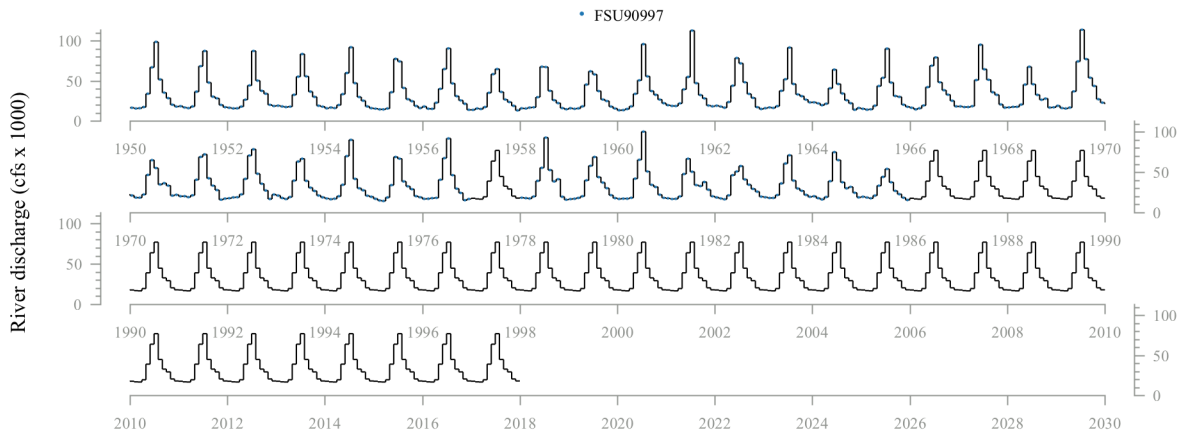
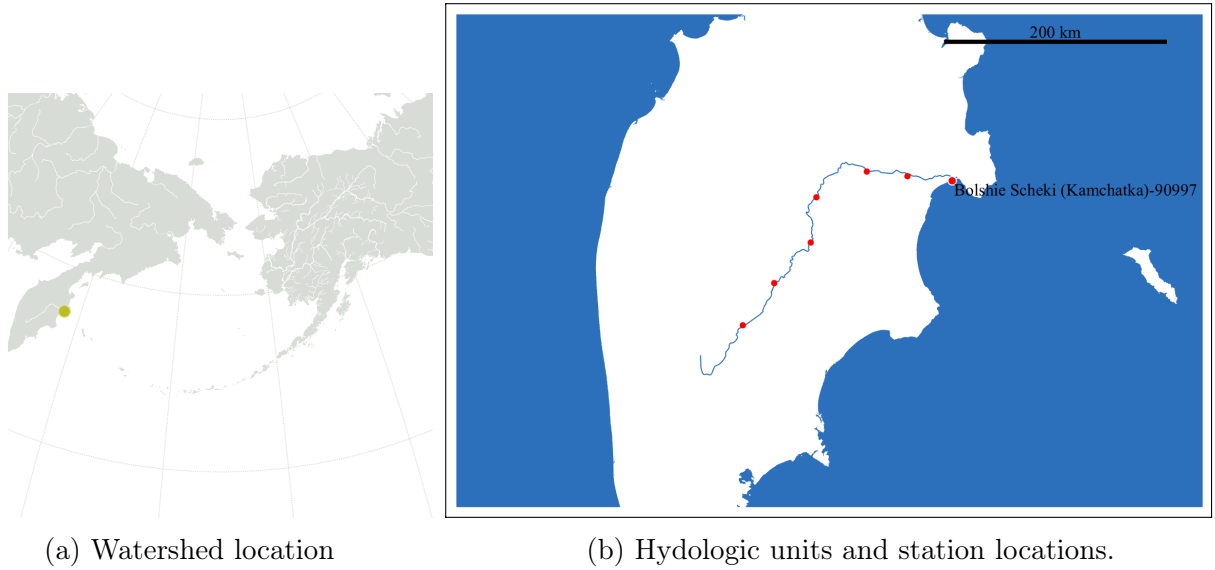


Figure A.26. -- The Former Soviet Union dataset included several stations along the Kamchatka River. We used data from station 90997, near the mouth of the river, which spanned the timeperiod of 1950 - 1988, and we extended beyond the measurement period with climatological averages.

## Avacha River

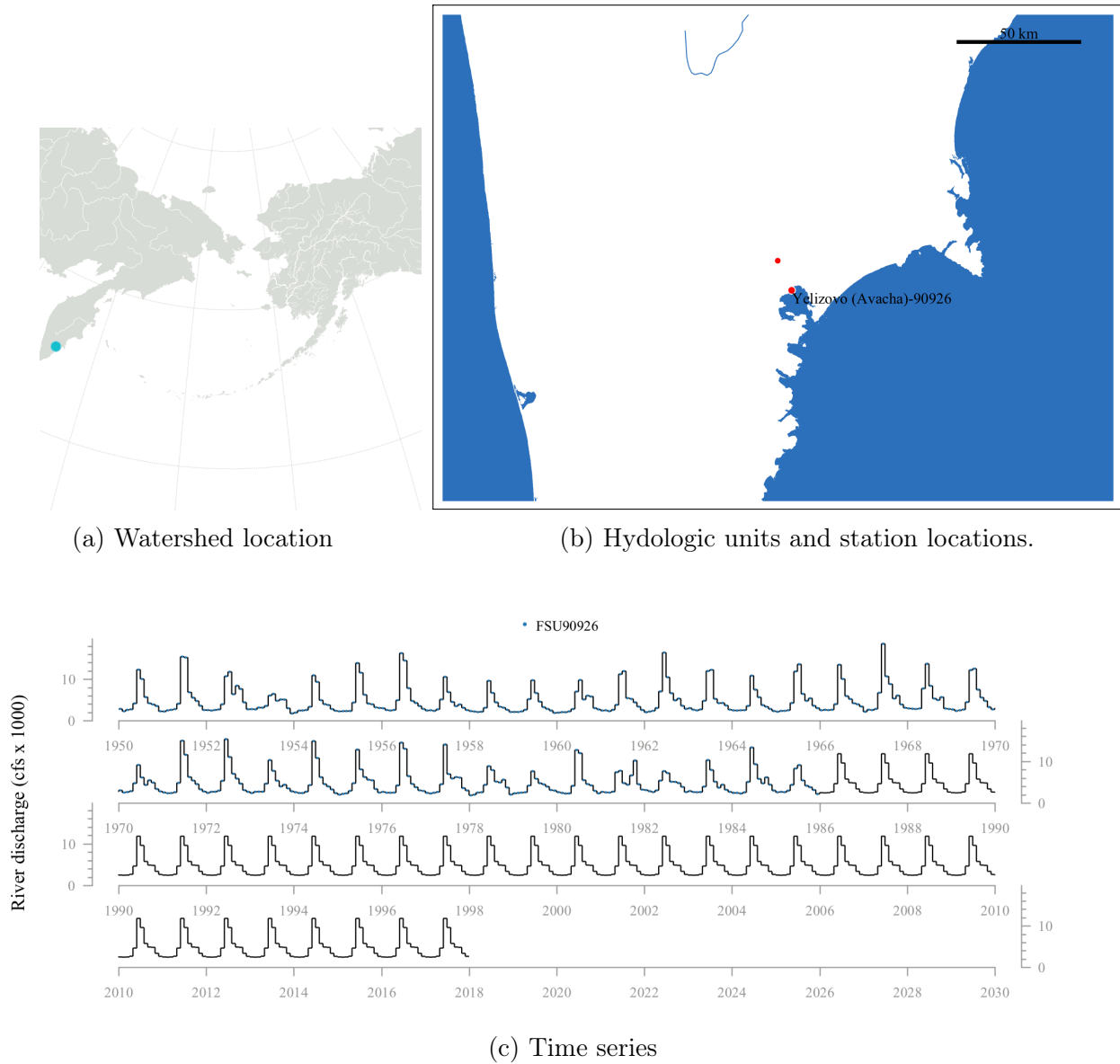


Figure A.27. -- The small Avacha River had two stations available along it. Data from station 90926 were used for 1950 - 1986, and climatological averages were used to extend data to the more recent years.

# Anadyr River

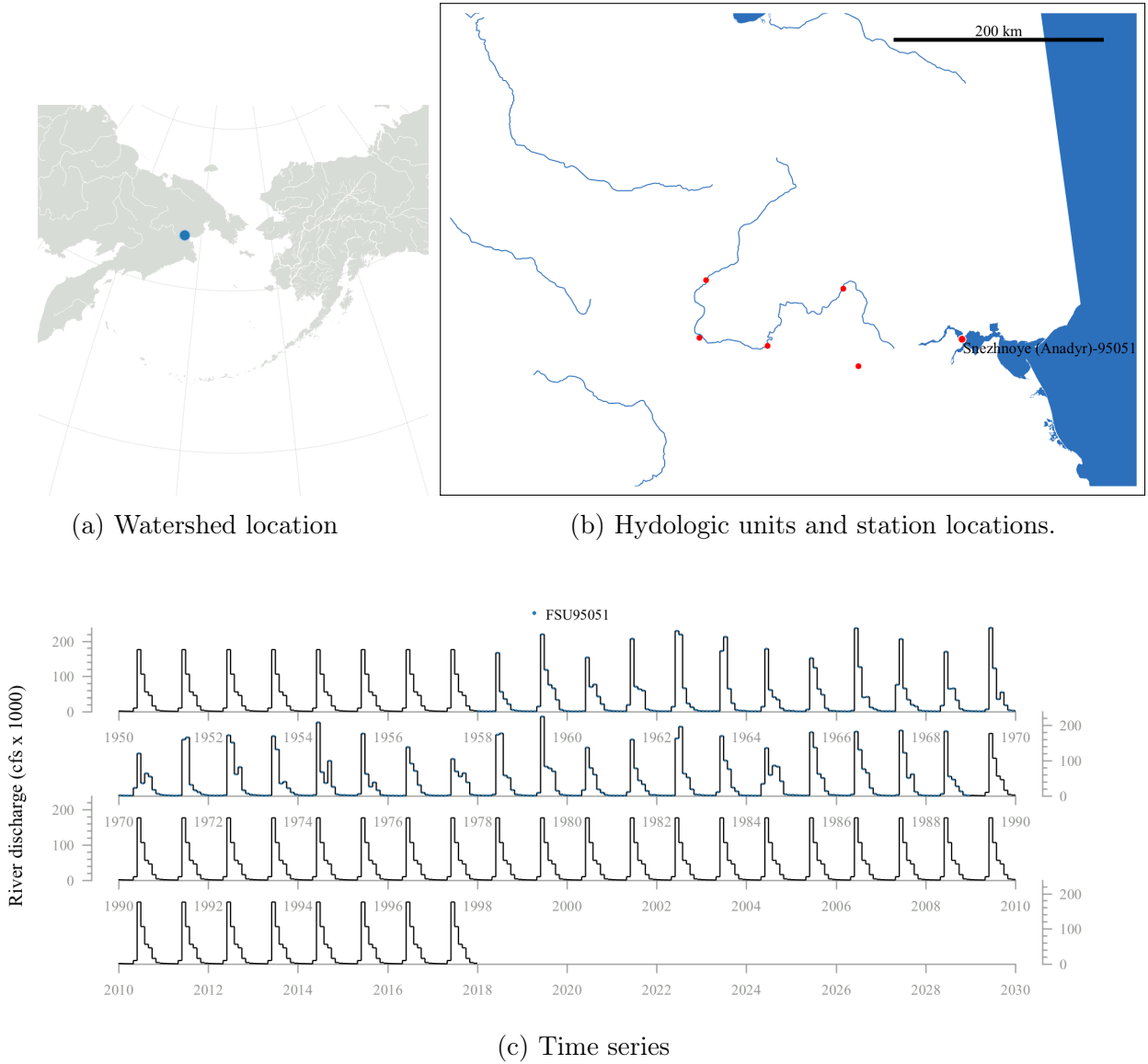


Figure A.28. -- The Anadyr River delivers the highest freshwater flux on the western side of the domain, and several monitoring stations were available along it. Data from the station 95051, located at the mouth of the river, was used for the period of 1958 - 1988, with a climatological average used for the earlier and later periods.

## RECENT TECHNICAL MEMORANDUMS

Copies of this and other NOAA Technical Memorandums are available from the National Technical Information Service, 5285 Port Royal Road, Springfield, VA 22167 (web site: [www.ntis.gov](http://www.ntis.gov)). Paper and electronic (.pdf) copies vary in price.

### AFSC-

- 387 FENSKE, K. H., A. M. BERGER, B. CONNORS, J.M. COPE, S. P. COX, M. A. HALTUCH, D. H. HANSELMAN, M. KAPUR, L. LACKO, C. LUNSFORD, C. RODGVELLER, and B. WILLIAMS. 2019. Report on the 2018 International Sablefish Workshop, 107 p. NTIS number pending.
- 386 LANG, C. A., J. I. RICHA, and R. J. FOY. 2019. The 2018 eastern Bering Sea continental shelf and northern Bering Sea trawl surveys: Results for commercial crab species, 220 p. NTIS No. PB2019-100298.
- 385 JEFFERSON, T. A., M. E. DAHLHEIM, A. N. ZERBINI, J. M. WAITE, and A. S. KENNEDY. 2019. Abundance and seasonality of Dall's porpoise (*Phocoenoides dalli*) in Southeast Alaska, 45 p. NTIS No. PB2019-100297.
- 384 RUSSELL, J. R., S. C. VULSTEK, J. E. JOYCE, R. P. KOVACH, and D. A. TALLMON. 2018. Long-term changes in length at maturity of Pacific salmon in Auke Creek Alaska, 28 p. NTIS No. PB2019-100295.
- 383 LEW, D. K., and J. LEE. 2018. Costs, earnings, and employment in the Alaska saltwater sport fishing charter sector, 2015, 85 p. NTIS No. PB2019-100296.
- 382 MCKELVEY, D., and K. WILLIAMS. 2018. Abundance and distribution of age-0 walleye pollock in the eastern Bering Sea shelf during the Bering Arctic Subarctic Integrated Survey (BASIS) in 2014, 48 p. NTIS No. PB2018-101437.
- 381 BRYAN, D. R., M. LEVINE, and S. MCDERMOTT. 2018. Results of the 2016 and 2017 Central and Western Aleutian Islands underwater camera survey of Steller sea lion prey fields, 87 p. NTIS No. PB2018-101436.
- 380 SEUNG, C. K., and S. MILLER. 2018. Regional economic analysis for North Pacific fisheries, 86 p. NTIS No. PB2018-101435.
- 379 GANZ, P., S. BARBEAUX, J. CAHALAN, J. GASPER, S. LOWE, R. WEBSTER, and C. FAUNCE. 2017. Deployment performance review of the 2016 North Pacific Groundfish and Halibut Observer Program, 68 p. NTIS No. PB2018-101537.
- 378 M. M. MUTO, V. T. HELKER, R. P. ANGLISS, B. A. ALLEN, P. L. BOVENG, J. M. BREIWICK, M. F. CAMERON, P. J. CLAPHAM, S. P. DAHLE, M. E. DAHLHEIM, B. S. FADELY, M. C. FERGUSON, L. W. FRITZ, R. C. HOBBS, Y. V. IVASHCHENKO, A. S. KENNEDY, J. M. LONDON, S. A. MIZROCH, R. R. REAM, E. L. RICHMOND, K. E. W. SHELDEN, R. G. TOWELL, P. R. WADE, J. M. WAITE, and A. N. ZERBINI. 2018. Alaska marine mammal stock assessments, 2017, 272 p. NTIS No. PB2018-101535.
- 377 RICHWINE, K. A., K. R. SMITH, and R. A. MCCONNAUGHEY. 2018. Surficial sediments of the eastern Bering Sea continental shelf: EBSSSED-2 database documentation, 48 p. NTIS No. PB2018-101013.